

Facile ZnO NPs catalyzed synthesis of substituted 4-amino-6-(1H-benzimidazol-2-ylsulfanyl)benzene-1,3-dicarbonitrile new derivatives as Potent biological agents

R. Champa^a, K. A. Vishnumurthy^b, Yadav D. Bodke^{c*}, H. S. BhojyaNaik^a, IttePushpavathi^a, N. D. Satyanarayan^d and B. N. Nippu^d

^aDepartment of P.G studies and research in Industrial Chemistry, Jnana Sahyadri, Shankaraghatta, Shivamogga, Karnataka-577451 India

^bDepartment of P.G studies and research in Industrial chemistry, Sir M V Govt. Science College, Bommanakatte, Bhadravathi, Shivamogga, Karnataka-577451 India

^cDepartment of P.G studies and research in Chemistry, Jnana Sahyadri, Shankaraghatta, Shivamogga, Karnataka-577451 India

^dDepartment of Pharmaceutical Chemistry, Kuvempu University, Post Graduate Centre, Kadur, Chikkamagaluru, 577548, Karnataka, India

CHRONICLE

Article history:

Received October 2, 2023

Received in revised form

January 5, 2024

Accepted February 8, 2024

Available online

February 8, 2024

Keywords:

Benzimidazole derivatives

Cytotoxicity

Antimicrobial

Anti-diabetic

DFT

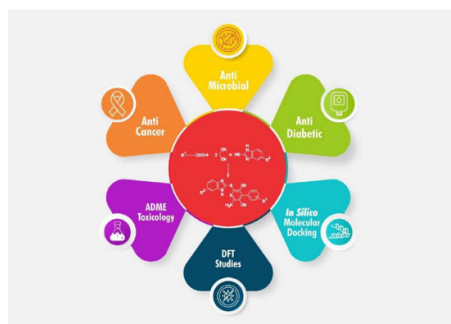
Molecular docking

ADME-toxicology study

ABSTRACT

This study focuses on the efficient synthesis of series of substituted 4-amino-6-(1H-benzimidazol-2-ylsulfanyl) benzene-1,3-dicarbonitrile derivatives synthesized from aldehydes, propanedinitrile, substituted thiols and catalyzed by ZnO nanoparticles (ZnONPs). All the synthesized compounds have been characterized using different spectroscopic techniques such as FT-IR, ¹H-NMR, C¹³-NMR and Mass. The compounds were evaluated for potential pharmacological applications, including antimicrobial, α-amylase inhibitory and anticancer activities. Computational calculations, DFT, *in-silico* molecular docking, and ADME-toxicology studies were performed. ADMET studies indicated that all synthesized compounds adhered to Rule of five with good bioavailability. This research underscores the promising pharmacological prospects of the synthesized newbenzimidazole derivatives.

© 2024 by the authors; licensee Growing Science, Canada.



Graphical Abstract

1. Introduction

4-Amino-6-(1H-benzimidazol-2-ylsulfanyl)benzene-1,3-dicarbonitrile derivatives are created by modifying the parent compound's structure while retaining its core chemical framework. The target compounds, 4-amino-6-(1H-benzimidazol-2-

* Corresponding author. Tel: +91-9449140275
E-mail address ydbodke@gmail.com (Y. D Bodke)

ylsulfanyl)benzene-1,3-dicarbonitrile derivatives, possess structural features that are often associated with biological activity¹. The presence of the benzimidazole moiety is known for its diverse pharmacological properties.

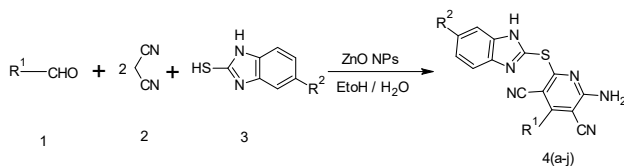
Benzimidazoles are a type of nitrogen containing heterocyclic molecules in which a benzene ring is fused to the 4 and 5 positions of an imidazole ring, also known as 1H-benzimidazole or 1,3-benzodiazole. It has been demonstrated that the functional group present in the benzimidazole molecule has a significant impact on the molecule's physical and chemical properties². Benzimidazole is an important heterocyclic template for significant research in chemical sciences due to their well-known uses and fascinating biological activity profile³⁻⁸. Benzimidazole is thought to be a physiologically active molecule with a wide range of biological properties, including antimicrobial⁹⁻¹³, anti-HIV¹⁴⁻¹⁷, anti-inflammatory and analgesic¹⁸⁻²⁰, antioxidant²⁰⁻²³, anticancer²³⁻²⁶, anti-diabetic²⁷, and anti-malarial^{20,28}.

The biological activity of benzimidazole derivatives is affected by both the type of substituent and the position at which it is linked to the benzimidazole ring²⁰. The mechanism for the biological activity of benzimidazole derivatives is complex and varies depending on the specific compound and its intended use. The electron-rich nitrogen heterocycles of benzimidazole could readily accept or donate protons and offer an advantage for it to bind with a broad spectrum of therapeutic targets, thereby exhibiting wide-ranging pharmacological activities²⁹. The presence of nitro-groups in organic molecules often enhances cycloaddition³⁰⁻³³ and additive bioactivity functions³⁴⁻³⁶ as they demonstrate vast efficacy in fighting bacteria, fungus, and parasites³⁷. Benzimidazole inhibits protein synthesis in microbes because benzimidazole has structural similarity with purine³⁸. The benzimidazole pharmacophore resembles naturally occurring purine nucleotides and exerts its biological activity through targeting specific molecules or non-gene-specific strategies²⁹. The physical and chemical properties of imidazoles and benzimidazoles, which are potential starting materials for a large number of important chemicals, are currently being actively studied². Benzimidazole compounds that are sold as pharmaceuticals include albendazole, omeprazole, pantoprazole, lansoprazole, rabeprazole, and tenatoprazole, as well as etonitazine, galeterone, mavatrep, and dovitinib^{39,40}. Benzimidazole is a favoured structure found in a variety of compounds with diverse biological functions, and it represents a number of important classes in drug discovery⁴¹⁻⁴⁶.

In general, the synthesis of 2-substituted benzimidazoles involves treating 1,2-phenylenediamines with carboxylic acids or their derivatives under intensely acidic conditions, which are sometimes paired with extremely high temperatures^{47,48}. These compounds are frequently produced by oxidatively combining phenylenediamines with aldehydes utilizing a variety of oxidative and catalytic reagents as well⁴⁹. Despite the effectiveness of the aforementioned conditions in promoting the reaction, they often involve homogeneous catalysts, and several of these methods exhibit one or more drawbacks. These drawbacks may include the use of stoichiometric or excessive amounts of reagents, the high cost of catalysts, extended reaction times, the occurrence of multiple side reactions, stringent reaction conditions, challenges in separating products from the reaction mixture, and the strong oxidizing nature of the reagents⁵⁰.

In light of benzimidazole's extensive pharmacological applications³⁸ and the need for an environmentally friendly process, this study constructed ten new 4-Amino-6-(1H-benzimidazol-2-ylsulfanyl)benzene-1,3-dicarbonitrile derivatives (4a-j) using ZnONPs as a catalyst in the synthetic route. The ZnONPs catalyzed approach offers advantages such as mild reaction conditions, eco-friendly and high yields as reported by number of researchers^{49,51-54}. Following the synthesis, a comprehensive evaluation of the pharmacological properties of the synthesized compounds was performed. This included investigating their potential antimicrobial, anticancer, and anti-diabetic activities. Additionally, we conducted computational studies utilizing molecular docking, ADMET and DFT studies to gain insights into the binding modes and interactions of these compounds with specific target proteins.

In this study, we carried out the synthesis of 4-amino-6-(1H-benzimidazole-2-ylsulfanyl) benzene-1,3-dicarbonitrile derivatives 4(a-j) through one pot reaction. Initially 10mL1:1(v/v) EtOH-H₂O was taken in a round bottom flask, an aldehyde(10mmol)(1) and propanedinitrile (20mmol)(2) added to start the reaction with stirring in presence of catalyst ZnONPs. The mixture was stirred at room temperature for 1 minute and then the substituted thiol (10mmol)(3) was added, refluxed for 2 hours⁵⁵ to get the desired solid product. The ZnO nanoparticle was synthesized according to the reported procedure by Davood Raoufi⁵⁶ The reaction pathway involved in the synthesis of target compounds (4a-j) has been given in **scheme 1**.



	4a	4b	4c	4d	4e	4f	4g	4h	4i	4j
R ¹	C ₆ H ₄ Cl ₂	C ₆ H ₇ N	C ₆ H ₅ NO ₂	C ₁₃ H ₁₂ O	C ₆ H ₅ F	C ₆ H ₄ Cl ₂	C ₆ H ₇ N	C ₆ H ₅ NO ₂	C ₁₃ H ₁₂ O	C ₆ H ₅ F
R ²	OCH ₃	OCH ₃	OCH ₃	OCH ₃	OCH ₃	CH ₃	CH ₃	CH ₃	CH ₃	CH ₃

Scheme 1. Synthesis of 4-amino-6-(1H-benzimidazol-2-ylsulfanyl)benzene-1,3-dicarbonitrile derivatives **4(a-j)**.

2. Results and Discussion

2.1. Synthesis

2.1.1. Synthesis of 2-amino-4-(2,4-dichlorophenyl)-6-((6-methoxy-1H-benzo[d]imidazol-2-yl)thio) pyridine-3,5-dicarbonitrile(4a)

In a 100 mL round bottom flask containing 10 mL 1:1(v/v) EtOH/H₂O, the 2,4-dichlorobenzaldehyde (10 m mol) (**1**), propanedinitrile(20m mol) (**2**), catalyst (ZnO NPs) were added with stirring at room temperature for 1min then 6-methoxy-1H-benzimidazole-2-thiol(10mmol)(**3**) was added and refluxed for 2hr to afford a solid compound (**4a**).

Yield: 98%.Light brown solid; mp: 158-160°C.IR(KBr, ν cm⁻¹) ;3101(N-H), 3048(Ar-CH), 2226(C=N), 1619(C=C), 1578(C-O); ¹H NMR (400 MHz, DMSO-d₆, δ ppm):3.32(s, 3H, OCH₃), 6.66-6.73(m, 3H, ArH), 7.03(d, $J=8$ Hz 1H, Ar-H), 7.71(dd, $J_1=8$ Hz $J_2=8$ Hz 1H, Ar-H),7.92-8.63(m, 1H,Ar-H , 2H, NH₂), 12.37(1H, NH).¹³C NMR (100 MHz, DMSO-d₆, δ ppm):55.50(OCH₃), 87.00(C-CH), 94.42, 109.6(C-N), 109.9, 112.1, 113.3, 126.3, 128.2, 128.5, 130.0, 130.8(C=C), 133.0, 135.3, 138.7(C-S), 155.7(C-NH₂), 156.6, 167.7(C=O).LCMS: m/z 467[M+1].Anal. Cald. For C₂₂H₁₃Cl₂N₅OS Found: C;56.66, H;2.81, N;15.02% Found: C;56.60, H;2.80, N;15.01%

2.1.2. Synthesis of 2-amino-4-(1H-indol-3-yl)-6-((6-methoxy-1H-benzo[d]imidazol-2-yl)thio) pyridine-3,5-dicarbonitrile(4b)

In a 100 mL round bottom flask containing 10 mL 1:1(v/v) EtOH/H₂O, the 1H-indole-3-carbaldehyde (10 m mol) (**1**), propanedinitrile(20m mol) (**2**), catalyst (ZnO NPs) were added with stirring at room temperature for 1min then 6-methoxy-1H-benzimidazole-2-thiol(10mmol) (**3**) was added and refluxed for 2hr to afford a solid compound (**4b**).

Yield: 96%.Light yellow solid; mp: 208-210°C.IR (KBr, ν cm⁻¹) ;2949(N-H), 2886(Ar-CH), 2216(C=N), 1633(C=C), 1590(C-O);¹H NMR (400 MHz, DMSO-d₆, δ ppm):3.34(s, 3H, OCH₃), 6.67-6.74(m, 2H, ArH), 7.03(d, $J=8$ Hz 1H, Ar-H), 7.38(m, 2H, Ar-H,),7.58(d, $J=8$ Hz 1H, Ar-H), 8.53-8.71(1H,Ar-H , 2H, NH₂), 12.72(s, 1H,NH).¹³C NMR (100 MHz, DMSO-d₆, δ ppm): 55.51(OCH₃), 69.26, 84.9(C-CH), 94.4, 109.6(C-N), 109.9, 110.9, 113.0, 115.8, 115.9, 119.0, 122.5, 123.9, 126.3, 126.6, 133.0(C=C), 133.2, 136.1(C-S), 152.5, 155.7(C-NH₂), 167.7(C=O).LCMS: m/z 437[M+1].Anal. Cald. For C₂₄H₁₆N₆OS C;56.66, H;2.81, N;15.02% Found: C;56.60, H;2.80, N;15.01%

2.1.3. Synthesis of 2-amino-6-((6-methoxy-1H-benzo[d]imidazol-2-yl)thio)-4-(3-nitrophenyl) pyridine-3,5-dicarbonitrile(4c)

In a 100 mL round bottom flask containing 10 mL 1:1(v/v) EtOH/H₂O, the 3-nitrobenzaldehyde (10 m mol) (**1**), propanedinitrile (20m mol) (**2**), catalyst (ZnO NPs) were added with stirring at room temperature for 1min then 6-methoxy-1H-benzimidazole-2-thiol(10mmol) (**3**) was added and refluxed for 2hr to afford a solid compound (**4c**)

Yield: 97%.Light brown solid; mp: 148-150°C.IR (KBr, ν cm⁻¹);3120(N-H), 3081(Ar-CH), 2228(C=N),1641(C=C),1572(C-O);¹H NMR (400 MHz, DMSO-d₆, δ ppm):3.41(s, 3H, OCH₃), 6.67-6.73(m, 2H, ArH), 7.03(d, $J=8$ Hz 2H, Ar-H), 7.89(t, $J=8$ Hz 1H,Ar-H),8.32(d, $J=8$ Hz 1H, Ar-H),8.47-8.73(m, 1H, Ar-H, 2H, NH₂),12.39(s, 1H,NH).¹³C NMR (100 MHz, DMSO-d₆, δ ppm):55.44(OCH₃), 84.82(C-CH), 94.40, 109.6(C-N), 109.9, 112.5, 113.6, 124.7, 126.3, 127.8, 131.0(C=C), 132.38, 133.0, 135.8(C-S), 147.9, 155.7(C-NH₂), 159.1, 167.7(C=O).LCMS: m/z 443[M+1].Anal. Cald. ForC₂₂H₁₄O₃S C;56.66, H;2.81, N;15.02% Found: C;56.60, H;2.80, N;15.01%

2.1.4. Synthesis of 2-amino-4-(3-(benzyloxy)phenyl)-6-((6-methoxy-1H-benzo[d]imidazol-2-yl)thio) pyridine-3,5-dicarbonitrile(4d)

In a 100 mL round bottom flask containing 10 mL 1:1(v/v) EtOH/H₂O, the 3-(benzyloxy)benzaldehyde (10 mmol) (**1**), propanedinitrile (20mmol) (**2**), catalyst (ZnO NPs) were added with stirring at room temperature for 1min then 6-methoxy-1H-benzimidazole-2-thiol(10mmol) (**3**) was added and refluxed for 2hr to afford a solid compound (**4d**)

Yield: 98%.Light yellow solid; mp: 138-140°C.IR (KBr, ν cm⁻¹);3300(N-H), 3060(Ar-CH), 2224(C=N),1621(C=C),1567(C-O);¹H NMR (400 MHz, DMSO-d₆, δ ppm):3.71(s, 3H, OCH₃), 5.13(s,2H, CH₂), 6.65-6.71(m, 3H, ArH), 7.01(d, $J=8$ Hz1H, Ar-H), 7.49-8.46(m, 4H, Ar-H, 2H, NH₂),12.37(s, 1H,NH).¹³C NMR (100 MHz, DMSO-d₆, δ ppm):55.50(OCH₃), 69.54, 81.88(C-CH), 94.41, 109.6(C-N), 109.9, 113.1, 114.1, 116.3, 120.8, 123.0, 126.3, 127.8, 128.0, 128.4, 130.7(C=C), 132.4, 133.0, 136.3(C-S), 155.7(C-NH₂), 158.5, 161.2, 167.7(C=O).LCMS: m/z 504[M+1].Anal. Cald. ForC₂₂H₁₄N₆O₃S C;56.66, H;2.81, N;15.02% Found: C;56.60, H;2.80, N;15.01%

2.1.5. *Synthesis of 2-amino-4-(4-fluorophenyl)-6-((6-methoxy-1H-benzo[d]imidazol-2-yl)thio)pyridine-3,5-dicarbonitrile(4e)*

In a 100 mL round bottom flask containing 10 mL 1:1(v/v) EtOH/H₂O, the 4-fluorobenzaldehyde (10 m mol) (**1**), propanedinitrile (20mmol) (**2**), catalyst (ZnO NPs) were added with stirring at room temperature for 1min then 6-methoxy-1H-benzimidazole-2-thiol(10mmol) (**3**) was added and refluxed for 2hr to afford a solid compound (**4e**)

Yield: 97%.Light yellow solid; mp: 148-150°C.IR (KBr, ν cm^{-1}):3300(N-H), 3059(Ar-CH), 2228(C=N),1639(C=C),1575(C-O);¹H NMR (400 MHz, DMSO-d₆, δ ppm):3.75(s, 3H, OCH₃), 6.68-6.74(m, 2H, ArH), 7.03(d,*J*=8Hz,1H, Ar-H), 7.49(t,*J*=8Hz, 2H,Ar-H), 8.04-8.53(3H, Ar-H, 2H, NH₂),12.35(1H,NH).¹³C NMR (100 MHz, DMSO-d₆, δ ppm): 55.50(OCH₃), 81.12(C-CH), 94.41, 109.6(C-N), 109.9, 113.1, 114.1, 116.7, 117.0, 126.3, 127.9, 128.0, 133.0(C=C), 133.46, 133.56(C-S), 155.7(C-NH₂), 160.1, 163.8, 166.4, 167.7(C=O).LCMS: m/z 416[M+1].Anal. Cald. For C₂₂H₁₄FN₅O S;56.66, H;2.81, N;15.02% Found: C;56.60, H;2.80, N;15.01%.

2.1.6. *Synthesis of 2-amino-4-(2,4-dichlorophenyl)-6-((6-methyl-1H-benzo[d]imidazol-2-yl)thio)pyridine-3,5-dicarbonitrile(4f)*

In a 100 mL round bottom flask containing 10 mL 1:1(v/v) EtOH/H₂O, the 2,4-dichlorobenzaldehyde (10 m mol) (**1**), propanedinitrile (20mmol) (**2**), catalyst (ZnO NPs) were added with stirring at room temperature for 1min then 6-methyl-1H-benzimidazole-2-thiol(10mmol) (**3**) was added and refluxed for 2hr to afford a solid compound (**4f**)

Yield: 98%.Light yellow solid; mp: 158-160°C.IR (KBr, ν cm^{-1}):3429(N-H), 3098(Ar-CH), 2220(C=N),1688(C=C),1580(C-O);¹H NMR (400 MHz, DMSO-d₆, δ ppm):2.34(s, 3H, CH₃), 6.98(dd, *J*₁=8Hz, *J*₂=8Hz, 3H, ArH), 7.72(dd,*J*₁=8Hz, *J*₂=8Hz, 2H, Ar-H), 8.05(d, *J*=8Hz 2H, Ar-H), 8.64(s, 2H, NH₂), 12.42(s,1H, NH).¹³C NMR (100 MHz, DMSO-d₆, δ ppm):20.9(CH₃), 87.1(C-CH), 94.41, 109.1(C-N), 109.6, 112.2, 113.3, 123.2, 128.3, 128.6, 130.0, 130.2, 130.3, 131.0, 131.6, 135.3(C=C), 138.7(C-S), 156.7(C-NH₂), 167.6(C=O).LCMS: m/z 451[M+1].Anal. Cald. For C₂₂H₁₃Cl₂N₅S C;56.66, H;2.81, N;15.02% Found: C;56.60, H;2.80, N;15.01%.

2.1.7. *Synthesis of 2-amino-4-(1H-indol-3-yl)-6-((6-methyl-1H-benzo[d]imidazol-2-yl)thio)pyridine-3,5-dicarbonitrile(4g)*

In a 100 mL round bottom flask containing 10 mL 1:1(v/v) EtOH/H₂O, the 1H-indole-3-carbaldehyde (10 m mol) (**1**), propanedinitrile (20mmol) (**2**), catalyst (ZnO NPs) were added with stirring at room temperature for 1min then 6-methyl-1H-benzimidazole-2-thiol(10mmol) (**3**) was added and refluxed for 2hr to afford a solid compound (**4g**)

Yield: 97%.Light yellow solid; mp: 219-220°C.IR (KBr, ν cm^{-1});3277(N-H), 2995(Ar-CH), 2220(C=N), 1602(C=C), 1565(C-O);¹H NMR (400 MHz, DMSO-d₆, δ ppm):2.34(s, 3H, CH₃), 6.98(dd, *J*₁=8Hz, *J*₂=8Hz, 1H, ArH), 7.047 to 7.60(m,7H, Ar-H), 7.36(m, 2H, Ar-H), 8.51(s, 2H, NH₂), 12.43(s, 1H, NH).¹³C NMR (100 MHz, DMSO-d₆, δ ppm):20.9(CH₃),87.1(C-CH), 109.1(C-N), 109.6, 110.0, 113.0, 115.9, 116.0, 119.0, 122.6, 123.2, 124.0, 126.7, 130.2, 131.6, 132.5, 133.2(C=C), 136.1(C-S), 152.5(C-NH₂), 167.7(C=O).LCMS: m/z 421[M+1].Anal. Cald. For C₂₄H₁₆N₆S C; 56.66, H;2.81, N;15.02% Found: C;56.60, H;2.80, N;15.01%.

2.1.8. *Synthesis of 2-amino-6-((6-methyl-1H-benzo[d]imidazol-2-yl)thio)-4-(3-nitrophenyl)pyridine-3,5-dicarbonitrile(4h)*

In a 100 ml round bottom flask containing 10 ml 1:1(v/v) EtOH/H₂O, the 3-nitrobenzaldehyde (10 m mol) (**1**), propanedinitrile(20m mol) (**2**), catalyst (ZnO NPs) were added with stirring at room temperature for 1min then 6-methyl-1H-benzimidazole-2-thiol(10mmol) (**3**) was added and refluxed for 2hr to afford a solid compound (**4h**)

Yield: 98%.Light brown solid; mp: 128-130°C.IR (KBr, ν cm^{-1}); 3377(N-H), 3080(Ar-CH), 2951(C=N),1601(C=C),1527(C-O);¹H NMR (400 MHz, DMSO-d₆, δ ppm):2.33(s, 3H, CH₃), 6.95(m, 1H, ArH), 7.96(t, *J*=8Hz 2H, Ar-H), 8.39(d, *J*=8Hz 2H,Ar-H), 8.32(d, *J*=8Hz 2H, Ar-H),8.77(s, 2H, NH₂),12.38(s, 1H,NH).¹³C NMR (100 MHz, DMSO-d₆, δ ppm): 20.9(CH₃), 84.8(C-CH), 109.1(C-N), 109.6, 112.6, 113.6, 123.1, 123.9, 124.8, 127.9, 128.5, 130.2, 130.9, 131.1, 131.6, 132.4, 132.4(C=C) 134.9, 135.8(C-S). 147.9, 159.2(C-NH₂), 167.7(C=O). LCMS: m/z 426[M+1].Anal. Cald. For C₂₂H₁₄N₆O₂S C;56.66, H;2.81, N;15.02% Found: C;56.60, H;2.80, N;15.01%.

2.1.9. *synthesis of 2-amino-4-(3-(benzyloxy)phenyl)-6-((6-methyl-1H-benzo[d]imidazol-2-yl)thio)pyridine-3,5-dicarbonitrile(4i)*

In a 100 mL round bottom flask containing 10 mL 1:1(v/v) EtOH/H₂O, the 3-(benzyloxy)benzaldehyde (10 m mol) (**1**), propanedinitrile(20m mol) (**2**), catalyst (ZnO NPs) were added with stirring at room temperature for 1min then 6-methyl-1H-benzimidazole-2-thiol(10mmol) (**3**) was added and refluxed for 2hr to afford a solid compound (**4i**)

Yield: 97%. Light yellow solid; mp: 138-140°C. IR (KBr, ν cm^{-1}): 3399(N-H), 3033(Ar-CH), 2958(C=N), 1639(C=C), 1572(C-O); ^1H NMR (400 MHz, DMSO- d_6 , δ ppm): 2.30(s, 3H, CH_3), 3.41(s, 2H, CH_2), 7.54(m, 2H, ArH), 7.27(m, 5H, Ar-H), 7.56(d, $J=8\text{Hz}$, 2H, Ar-H), 8.00(d, $J=8\text{Hz}$, 2H, Ar-H), 8.52(s, 1H, Ar-H), 8.66(s, 2H, NH_2), (12.41(s, 1H, NH). ^{13}C NMR (100 MHz, DMSO- d_6 , δ ppm): 20.9(CH_3), 69.5, 81.8(C-CH), 94.40, 109.1(C-N), 109.6, 113.1, 114.1, 116.3, 120.8, 123.0, 123.1, 127.8, 128.0, 128.5, 130.2, 130.7, 131.6, 132.4(C=C), 136.3(C-S), 158.5(C-NH $_2$), 161.2, 167.7(C=O). LCMS: m/z 487[M+1]. Anal. Calcd. For $\text{C}_{28}\text{H}_{20}\text{N}_6\text{OS}$ C;68.83, H;4.13, N;17.20, O;3.27, S;6.56% Found: C;68.73, H;4.10, N;17.10, O;3.20, S;6.50%.

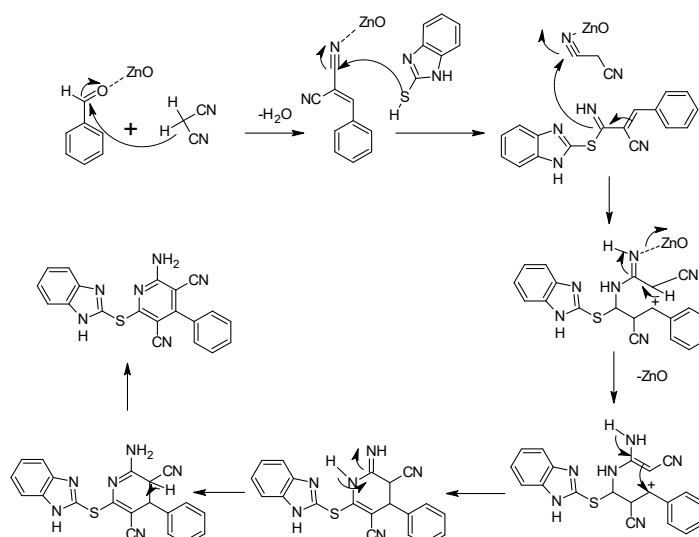
4.2.2. synthesis of 2-amino-4-(4-fluorophenyl)-6-((6-methyl-1H-benzo[d]imidazol-2-yl)thio) pyridine-3,5-dicarbonitrile(4j)

In a 100 mL round bottom flask containing 10 mL 1:1(v/v) EtOH/ H_2O , the 4-fluorobenzaldehyde (10 mmol) (**1**), propanedinitrile (20mmol) (**2**), catalyst (ZnO NPs) were added with stirring at room temperature for 1min then 6-methyl-1H-benzimidazole-2-thiol(10mmol) (**3**) was added and refluxed for 2hr to afford a solid compound (**4j**)

Yield: 98%. Light yellow solid; mp: 148-150°C. IR (KBr, ν cm^{-1}): 3110(N-H), 3059(Ar-CH), 2235(C=N), 1630(C=C), 1595(C-O); ^1H NMR (400 MHz, DMSO- d_6 , δ ppm): 2.34(s, 3H, CH_3), 6.97(m, 3H, ArH), 7.50(m, 2H, Ar-H), 8.05(m, 2H, Ar-H), 8.54(s, 2H, NH_2), 12.42(s, 1H, NH). ^{13}C NMR (100 MHz, DMSO- d_6 , δ ppm): 20.34(CH_3), 81.1(C-CH), 109.1(C-N), 109.60, 113.1, 114.1, 116.8, 117.0, 123.1, 128.0, 130.2, 131.6, 132.4, 133.5(C=C), 133.6(C-S), 160.1(C-NH $_2$), 163.9, 166.4, 167.7(C=O). LCMS: m/z 399[M+1]. Anal. Calcd. For $\text{C}_{22}\text{H}_{14}\text{FN}_5\text{S}$ C;56.66, H;2.81, N;15.02% Found: C;56.60, H;2.80, N;15.01%.

2.2. Chemistry

The possible mechanism for some new 4-amino-6-(1H-benzimidazol-2-ylsulfanyl)benzene-1,3-dicarbonitrile derivatives (**4(a-j)**) as shown in **Scheme 1.1**.⁵⁵ All the obtained derivatives are represented in **Fig. 1**.



Scheme 1.1: General mechanism of synthesis of 4-amino-6-(1H-benzimidazol-2-ylsulfanyl)benzene-1,3-dicarbonitrile derivatives

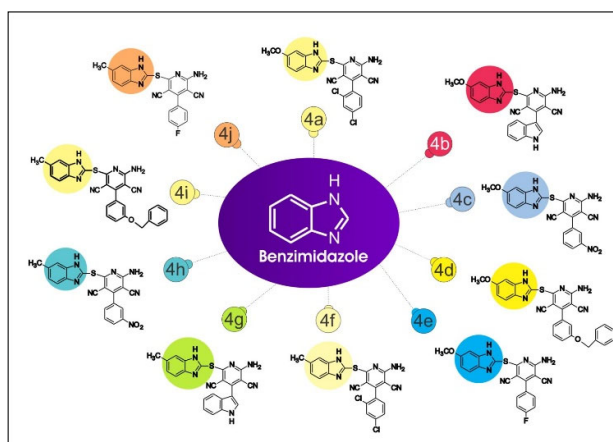


Fig. 1. 4-amino-6-(1H-benzimidazol-2-ylsulfanyl) benzene 1,3 dicarbonitrile derivatives **4(a-j)**

2.3. Pharmacological activities

2.3.1. Anti-microbial activity

All the synthesized compounds were evaluated for their *in vitro* antimicrobial activity against two bacterial strains (*Staphylococcus aureus* MTCC-7443 and *Escherichia coli* MTCC-7410), as well as two fungal species (*Aspergillus flavus* MTCC-9606 and *Pichia anomala* MTCC-237) and results are tabulated in **Table 1**. Zone of inhibition for different microorganisms was recorded for all the compounds at concentrations 20, 40, 60 and 80 µg; Rifampicin (30 µg) and fluconazole (30 µg) served as a positive control against bacteria and fungi respectively while DMSO as a negative control. In this study, zone of inhibition values of the studied compounds were investigated to detect their antibacterial and antifungal activities, and thus to determine the sensitivity of the microorganisms. The antimicrobial properties of the synthesized derivatives (**4a-j**) are tabulated in **Table 1**. It was found that compounds **4c** and **4h** were exhibited higher antimicrobial effect against all the strains of bacteria and fungi (*S. aureus*, *E. coli*, *A. flavus* and *P. anomala*) compared to other compounds and equivalent to standard antibiotic at higher concentration of 80 µg. It was noticed that *S. aureus*, *E. coli*, *A. flavus* and *P. anomala* found to be resistant to compounds **4b**, **4e**, **4i** and **4j** at different concentrations (20, 40, 60 and 80 µg). All other compounds exhibited significantly lesser antimicrobial effects than the standard antibiotic rifampicin and fluconazole (p value <0.01). Since the late 1990s and early 2000s, the antibacterial potential of the benzimidazole moiety has been widely explored, and numerous compounds have showed significant antimicrobial activity due to the presence of electron withdrawing groups⁵⁷. The benzimidazole scaffold which present in these derivatives contributes to their antimicrobial properties²⁰

Table 1. Antimicrobial activities of the synthesized compounds **4(a-j)**

Sl.	Sample Name	Conc. µg	<i>S. aureus</i>	<i>E. coli</i>	<i>A. flavus</i>	<i>P. anomala</i>
1	4a	40	5.33±0.58*	0±0	5.33±0.58*	0±0
		40	5.33±0.58*	0±0	5.33±0.58*	0±0
		60	9.33±0.58*	5.33±0.58	9.33±0.58*	0±0
		80	10.67±1.15*	7.67±0.58	10.67±1.15*	0±0
2	4b	60	0±0	5.33±0.58	0±0	0±0
		80	0±0	6.67±0.58	0±0	0±0
3	4c	20	5.67±0.58*	6.33±0.58	5.67±0.58*	0±0
		40	10.33±0.58*	10.67±0.58*	10.33±0.58*	0±0
		60	12.33±0.58*	13.33±0.58*	12.33±0.58*	6.33 ± 1.52*
		80	13.67±0.58*	15.67±0.58*	13.67±0.58*	10.33 ± 1.52*
4	4d	40	0±0	5.33±0.58*	0±0	0±0
		60	5.33±0.58*	6.33±0.58*	5.33±0.58*	0±0
		80	6.67±0.58*	8.33±0.58*	6.67±0.58*	0±0
5	4e	60	0±0	6.33±0.58*	0±0	0±0
		80	0±0	7.33±0.58*	0±0	0±0
8	4h	20	5.33±0.58*	5.67±0.58*	5.33±0.58	0±0
		40	7.67±0.58*	7.67±0.58*	7.67±0.58*	5.66 ± 0.57*
		60	9.33±0.58*	9.67±0.58*	9.33±0.58*	10.33 ± 1.52*
		80	12.67±0.58*	12.67±0.58*	12.67±0.58*	13.33 ± 1.15
9	4i	80	0±0	7.33±0.58*	0±0	0±0
10	4j	60	0±0	7.67±0.58*	0±0	0±0
		80	0±0	10.33±0.58*	0±0	0±0
	Rifampicin	30	25.33 ± 1.15	25.33 ± 0.57	--	--
	Fluconazole	30	--	--	14.33 ± 0.57	12.33 ± 0.57

* p value <0.001 for test compounds Vs standard antibiotics; n=3;

2.3.2. *In vitro* α-amylase inhibitory activity

All the synthesized compounds **4(a-j)** were screened for *in vitro* α-amylase inhibitory activity using different concentrations (20, 40, 60, 80 and 100 µg/mL) and acarbose was used as a standard for comparison. The α-amylase enzyme activity results revealed that, obtained compounds among all the derivatives **4a** and **4c** possessed highest inhibition efficacies of 56.36% and 67.82% respectively with respect to their concentration at 100 µg/mL as compared to standard at same concentration (90.11%). **Fig. 2** exhibits the percent inhibition of different compounds with varying concentrations (20, 40, 60, 80 and 100 µg/mL). The potencies of IC₅₀ values varying from 0 to 166.57±3.63 µg/mL. Among all compounds, **4g**, **4i** and **4j** exhibited no inhibition and compound **4c** exhibited good IC₅₀ value of 72.59±2.25 µg/mL as compared to standard drug acarbose (52.33±1.89 µg/mL) (**Fig. 3**). The results are shown in **Table 2**. The compounds **4a** and **4c** show excellent α-amylase inhibitory activity. The presence of electron withdrawing nitro and chloro groups in their ring structure may be the possible reason for the admirable anti-diabetic activity. These structural features can potentially interact with the active site of α-amylase, interfering with its catalytic activity and inhibiting the breakdown of carbohydrates⁵⁸.

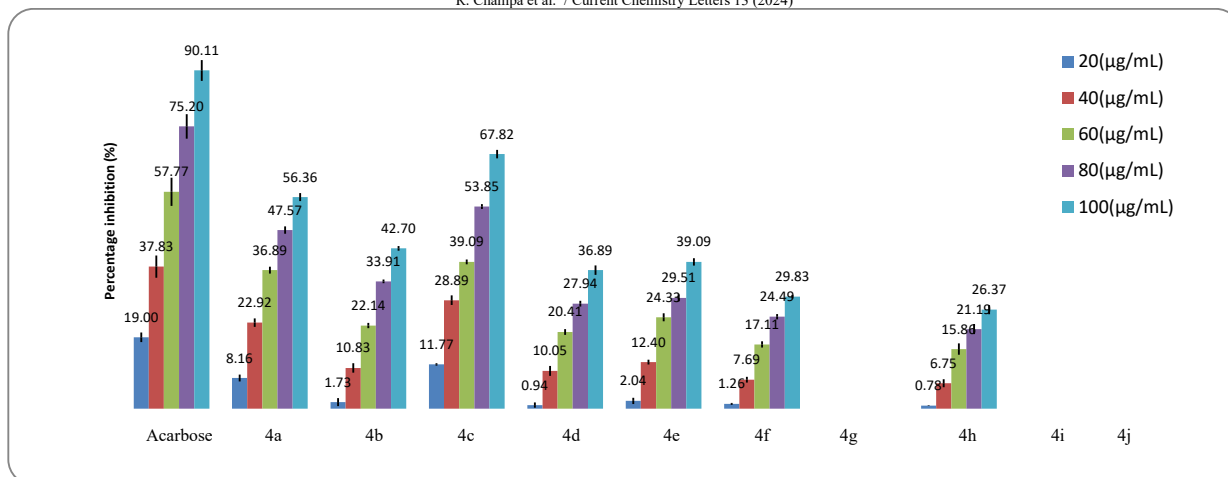


Fig. 2. *In vitro* α -amylase inhibitory activity of the synthesized derivatives **4(a-j)**-A graph of % inhibition of synthesized compounds at different concentration

Table 2. α -amylase enzyme activity results of the synthesized compounds **4(a-j)**

Sample	Concentration ($\mu\text{g/mL}$)					IC ₅₀
	20	40	60	80	100	
Acarbose	19 \pm 1.27	37.83 \pm 2.98	57.77 \pm 3.77	75.2 \pm 3.27	90.11 \pm 2.77	52.33 \pm 1.89
4a	8.16 \pm 0.91*	22.92 \pm 1.13*	36.89 \pm 0.91*	47.57 \pm 0.98*	56.36 \pm 1.06*	83.4 \pm 3.40*
4b	1.73 \pm 1.06*	10.83 \pm 1.27*	22.14 \pm 0.70*	33.91 \pm 0.49*	42.7 \pm 0.63*	110.41 \pm 3.41*
4c	11.77 \pm 0.32*	28.89 \pm 1.27*	39.09 \pm 0.63*	53.85 \pm 0.63*	67.82 \pm 1.13*	72.59 \pm 2.25*
4d	0.94 \pm 0.70*	10.05 \pm 1.34*	20.41 \pm 0.77*	27.94 \pm 0.77*	36.89 \pm 1.27*	126.75 \pm 2.47*
4e	2.04 \pm 0.84*	12.4 \pm 0.63*	24.33 \pm 1.06*	29.51 \pm 0.91*	39.09 \pm 0.98*	94.37 \pm 3.35*
4f	1.26 \pm 0.26*	7.69 \pm 0.77*	17.11 \pm 0.84*	24.49 \pm 0.70*	29.83 \pm 0.49*	148.88 \pm 4.08*
4g	0 \pm 0	0 \pm 0	0 \pm 0	0 \pm 0	0 \pm 0	0 \pm 0
4h	0.78 \pm 0.09*	6.75 \pm 1.07*	15.86 \pm 1.52*	21.19 \pm 1.35*	26.37 \pm 1.21*	166.57 \pm 3.63*
4i	0 \pm 0	0 \pm 0	0 \pm 0	0 \pm 0	0 \pm 0	0 \pm 0
4j	0 \pm 0	0 \pm 0	0 \pm 0	0 \pm 0	0 \pm 0	0 \pm 0

Values are Mean \pm Std, N=3, *P<0.01 vs. Control

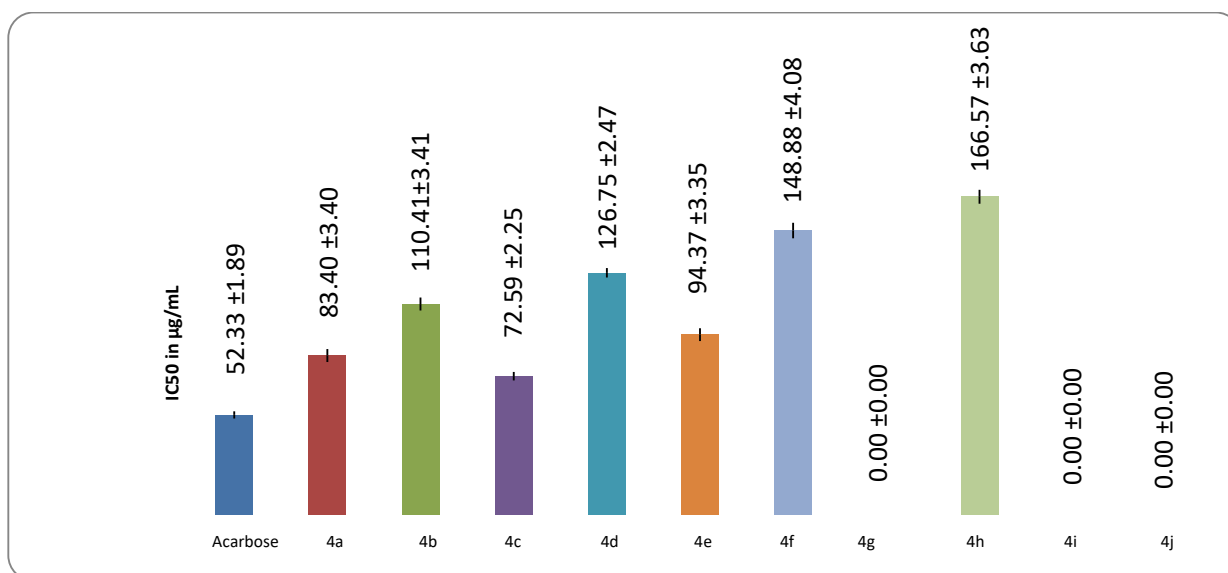


Fig. 3. *In vitro* α -amylase inhibitory activity of the synthesized compounds **4(a-j)**-A graph of IC₅₀ value of compounds

2.3.3. *In vitro* cytotoxicity

In vitro cytotoxicity was evaluated against the Human liver tumour cell line HepG2. A graph describing the concentrations versus cell inhibition of the derivatives were plotted (**Fig. 4**). Doxorubicin was used as reference standard for comparison. Significantly higher percent of inhibition (86.72 \pm 1.08%) was exhibited by compound **4c** when compared

to standard doxorubicin at concentration of 50µg/ml (73.82±0.27%). The activity result revealed that, synthesized compounds exhibited good sensitivity against the Hep G2 cell line with IC₅₀ values ranging from 21.12±1.59 to 74.17±3.07µg/mL (**Figure5**). Among them, the compound **4c** and **4h** shows significant cytotoxicity effect with good IC₅₀ value of 21.12±1.59 and 28.05±1.48 µg/mL as compared to reference standard doxorubicin (16.62±0.34µg/mL) and the obtained results were listed in **Table 3**. Suppression of genotoxic effects, improved antioxidant and anti-inflammatory activities, suppression of proteases and cell proliferation, protection of intracellular communications to modify apoptosis and signal transduction pathways may all be part of the preventative strategy⁵⁹. The compound **4c** shows significant cytotoxic effect, due to the presence of electron withdrawing groups in their ring structure, the presence of electron withdrawing group is assumed to be the key explanation for the compounds' remarkable anticancer activity⁶⁰.

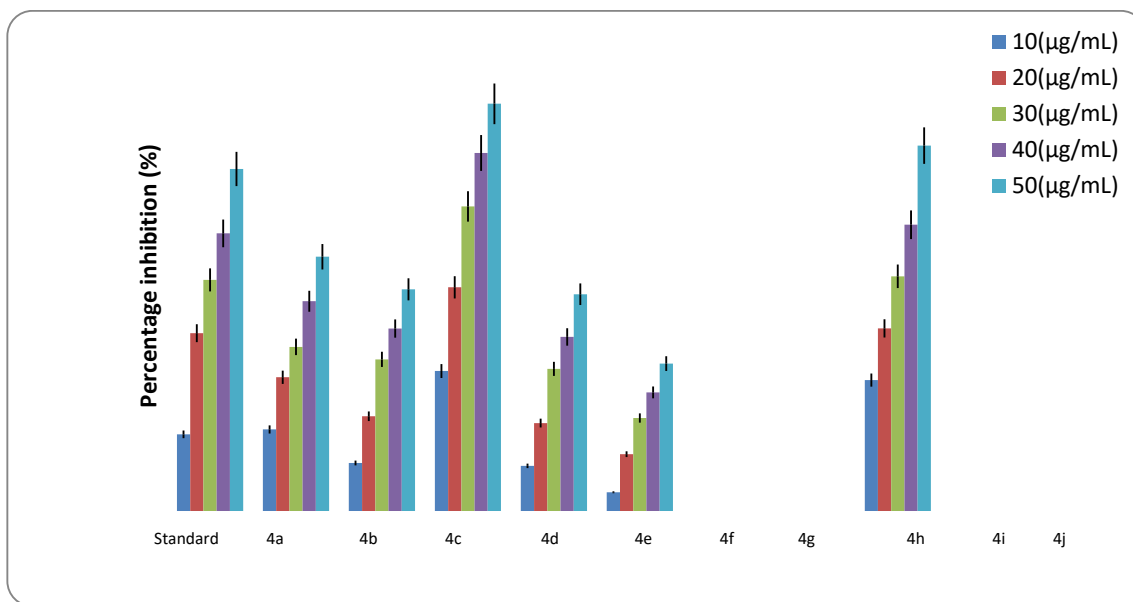


Fig. 4. A graph of percentage inhibition of cells by synthesized derivatives **4(a-j)** at different concentration against HEP G2 cell line

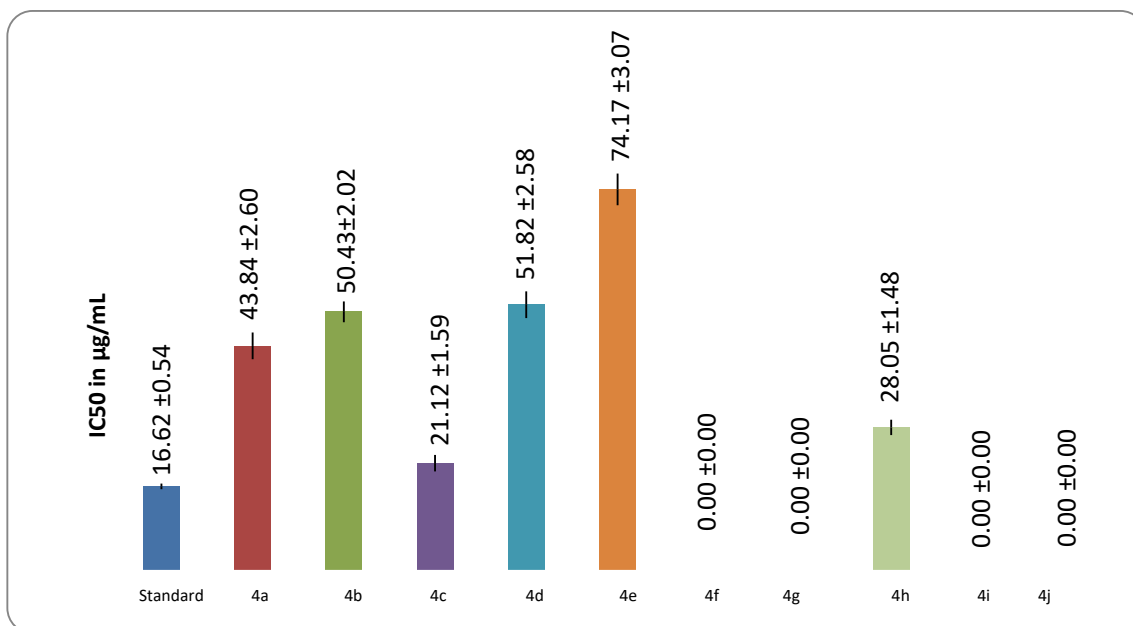


Fig. 5. A graph of IC₅₀ value of compounds **4(a-j)** against Hep G2 cell line

Table 3. Percentage of cell inhibition against Hep G2 (Human liver cancer cell line) cell line results of the synthesized compounds **4(a-j)**

Sample	Mean percentage inhibition of Hep G2(Human liver cancer cell line)					IC ₅₀
	Concentration (µg/mL)					
	10	20	30	40	50	
Standard	16.33±0.98	37.87±1.08	49.23±0.89	59.13±0.47	72.83±0.27	16.62±0.54
4a	17.36±0.53	28.48±0.36	34.96±0.62	44.67±1.00	54.15±0.81	43.84±2.60*
4b	10.23±0.53	20.18±0.36	32.29±0.54	38.85±0.17	47.21±0.44	50.43±2.02*
4c	29.80±0.80	47.63±0.26	64.85±0.54	76.26±0.73	86.72±1.08	21.12±1.59*
4d	9.62±0.37	18.72±0.54	30.27±0.54	37.07±1.53	46.18±0.97	51.82±2.58*
4e	3.99±1.11	12.11±0.44	19.80±0.47	25.25±0.67	31.39±0.17	74.17±3.07*
4f	0±0	0±0	0±0	0±0	0±0	0±0
4g	0±0	0±0	0±0	0±0	0±0	0±0
4h	27.87±0.89	38.90±0.62	49.98±0.54	60.96±0.47	77.80±1.00	28.05±1.48*
4i	0±0	0±0	0±0	0±0	0±0	0±0
4j	0±0	0±0	0±0	0±0	0±0	0±0

Standard-Doxorubicin; Values are in Mean ±STD, N=3, *P<0.01 vs. Standard

2.4. *In silico* molecular docking studies

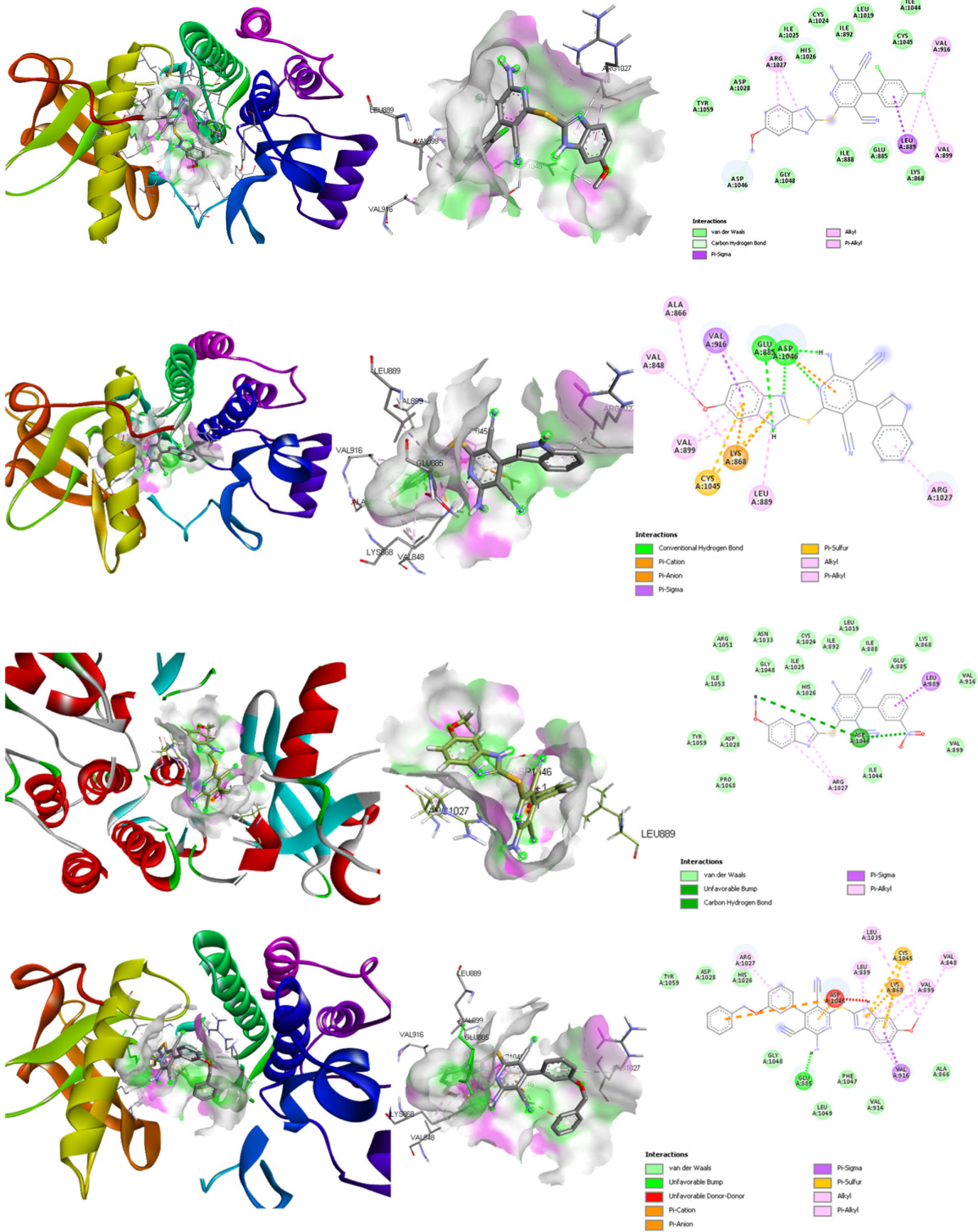
We have screened the synthesized compounds **4(a-j)** for *in silico* molecular docking studies as the study of intermolecular interactions between synthesized compounds and enzyme are necessary for the development of novel therapeutic drugs⁶¹. Molecular docking helps to predict the binding modes of the compounds with enzymes. Using HIF alpha as a target protein, the *in vitro* anticancer effects of benzimidazole derivatives were validated using *in silico* molecular docking simulation studies. HIF-1 functions as a transcription factor, upregulating genes involved in cell survival, angiogenesis, cancer progression, glucose metabolism, and metastasis, among other things. Currently, 60 putative HIF-1 target genes have been identified. Furthermore, HIF-1 targets proteins involved in the upregulation of Reactive Oxygen Species (ROS) and inflammation⁶². As a result, HIF-1 regulation is regarded as an important therapeutic target in the current study. The binding energy, number of hydrogen bonds, hydrophobic interactions, and docking score (affinity) of the synthesized compounds were compared to Axitinib. According to the *in silico* studies, all of the synthesized compounds have the nearest binding energy when compared to Axitinib.

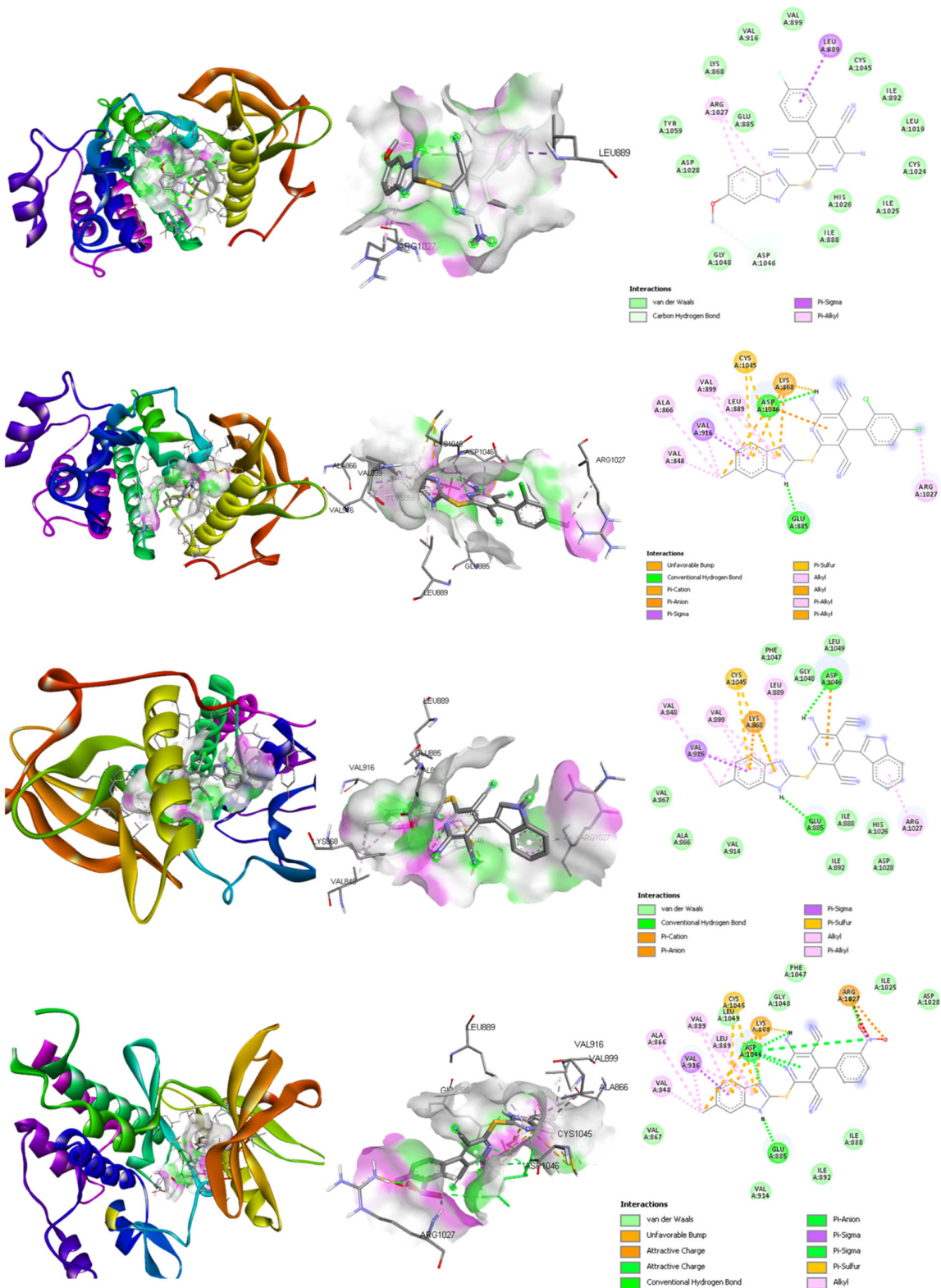
Table 4. Docking results of **4(a-j)** compounds against VEGFR2

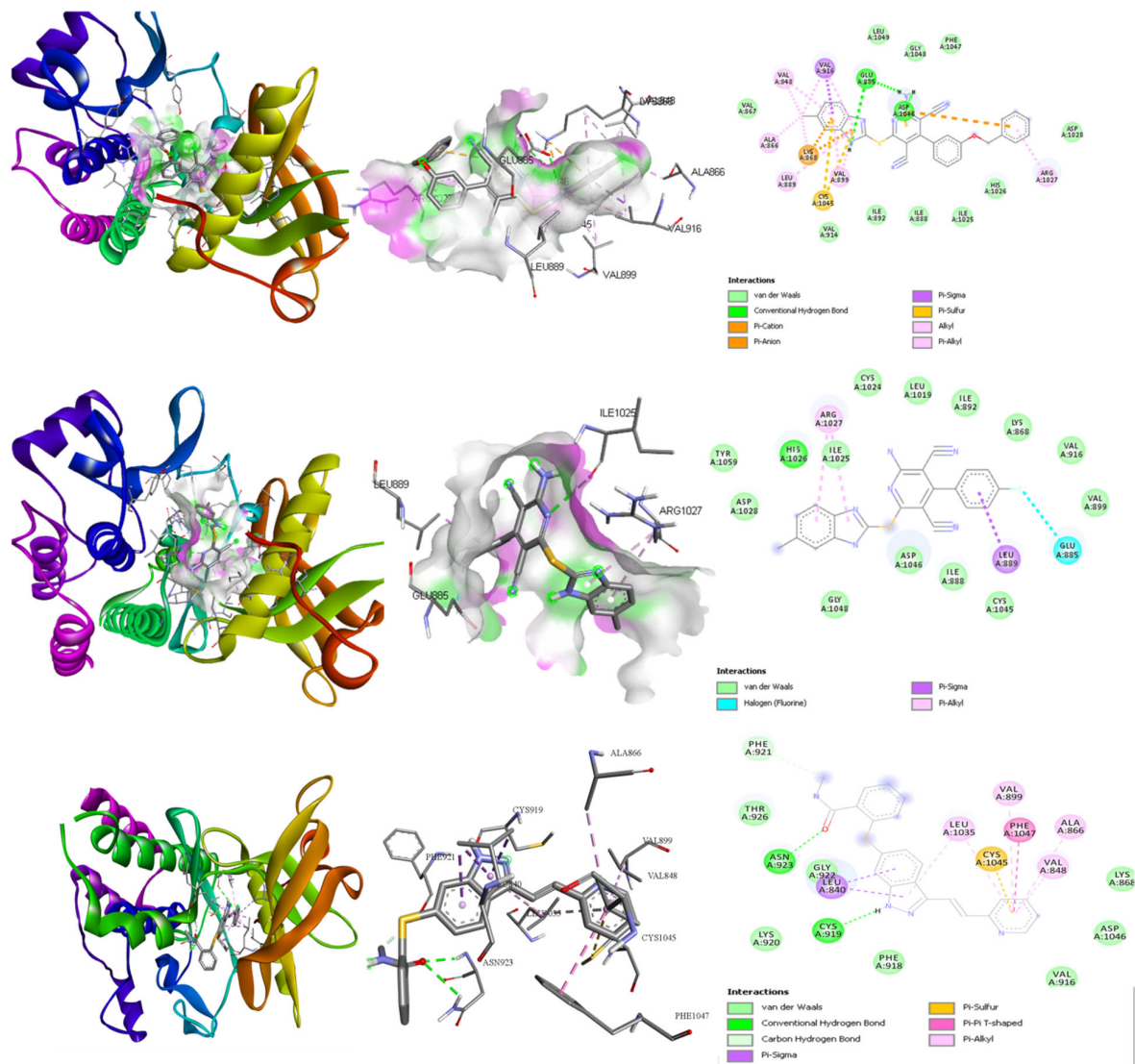
Ligand	Binding affinity (kcal/mol)	Hydrogen bond interaction	Hydrogen Bond length in Å	Electrostatic interaction	Hydrophobic and Other interactions
4a	-7.4	ASP1046	2.38	-	ARG1027, LEU889, VAL899, VAL916, ASP1028, HIS1026, LYS868, GLU885
4b	-7.0	ASP1046, GLU885	2.21, 2.33, 2.58, 2.30	LYS868	CYS1045, ARG1027, LEU889, VAL916, ALA866, VAL848, ASP1028, HIS1026
4c	-7.2	ASP1046	2.12	-	ARG1027, LEU889, VAL899, VAL916, ASP1028, HIS1026, LYS868, GLU885
4d	-7.1	GLU885	2.18	LYS868	CYS1045, ARG1027, LEU889, VAL916, ALA866, VAL848, ASP1028, HIS1026, LYS1023
4e	-7.3	ASP1046	2.36	-	CYS1045, ARG1027, LEU889, VAL916, ALA866, VAL848, ASP1028, HIS1026, LYS1023
4f	-7.2	ASP1046, GLU885	2.22, 2.48	ASP1046, LYS868	CYS1045, ARG1027, CYS1045, ARG1027, LEU889, VAL916, ALA866, VAL848, ASP1028, HIS1026
4g	-7.2	ASP1046, GLU885	2.63, 2.18, 2.36	LYS868	CYS1045, ARG1027, LEU889, VAL916, ALA866, VAL848, ASP1028, HIS1026
4h	-7.0	GLU885, ASP1046	2.87, 2.58, 2.71	LYS868, ARG1027	CYS1045, ARG1027, LEU889, VAL916, ALA866, VAL848, ASP1028, HIS1026, VAL914, ILE892, ILE915
4i	-7.8	GLU885, ASP1046	2.89, 2.98, 2.53	LYS868, ASP1046	CYS045, VAL899, LEU889, ALA866, VAL848, VAL916, ARG1027, HIS1026, ILE1025, ILE888
4j	-7.0	-	-	GLU885	LEU889, LYS868, ARG1027, ASP1046, HIS1026, LYS868
Axitinib	-9.5	ASN923, CYS919, PHE921	2.46, 2.55, 2.56	CYS1045	PHE1047, VAL899, ALA866, VAL848, LEU1035, LEU840, THR926, ASP1046

Table 4 shows the compounds' binding affinities, hydrogen bonds, and hydrophobic interactions. The binding affinities of all benzimidazole derivatives ranged from -7.0 to -7.8Kcal/mol. **4i** had the highest binding affinity with TNF-, with a binding energy of -7.8Kcal/mol and 3 hydrogen bonds. CYS045, VAL899, LEU889, ALA866, VAL848, VAL916, ARG1027, HIS1026, ILE1025 and ILE888 were the most abundant amino acids in hydrophobic interactions. **Table 5** depicts the 2D and 3D interactions of ligand and protein. Chronic inflammation is frequently linked to a number of degenerative diseases, including cancer, diabetes, and cardiovascular disease⁶³. Inhibiting this protein is considered to be a prominent strategy in treating several types of Cancer⁶⁴.

Table 5. 2D and 3D interactions of ligand and protein
Protein ligand interaction







2.5. DFT studies

Tables 6-8 show theoretically designed optimized structures, E HOMO, E LUMO levels as well as MEP structures. **Table 9** shows their respective energy level values, to provide a direct understanding of their optimized electronic structure. The frontier orbitals HOMO and LUMO are electron donors and acceptors, respectively. The distribution of red and green colours in the molecular orbital wave function represented the positive and negative phases. Frontier molecular orbitals (FMOs) containing the highest occupied molecular orbital (HOMO) and lowest unoccupied molecular orbital (LUMO), as well as the energy gap ($\Delta E = E_{\text{HOMO}} - E_{\text{LUMO}}$) were considered to be very effective parameters in chemical quantum chemistry⁶⁵. FMOs also delivered important information about chemical reactivity, biological activity and kinetic stability of the molecules⁶⁶. The optimized HOMO and LUMO structures of synthesized compounds (**4a-j**) are shown in **Table 6** and **7**.

DFT results reveal that, the energy gap (ΔE) of compounds **4(a-j)** in the range of 2.84 eV to 3.59 eV. In that, the compound **4c** showed less energy gap at 2.84 eV and more softness value (0.70 eV). Hence, compound **4c** was chemically more reactive compared to other molecules. Also, **4c** compound had more electronegative value of 1.42 eV, due to the presence of an electron-withdrawing nitro group on phenyl ring. Therefore, it has greater tendency to attract a bonding electron pair compared to other molecules. A smaller energy gap influences the chemical reactivity and polarizability of the title molecules⁶⁷⁻⁶⁹. The low electrophilicity index indicates the less toxicity of the synthesized compounds⁷⁰.

Table 6. The optimized molecular structures of compounds **4(a-j)**

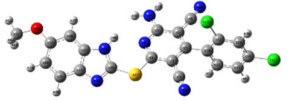
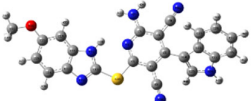
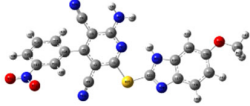
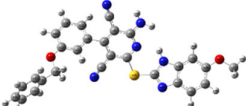
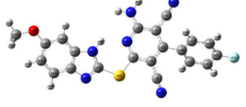
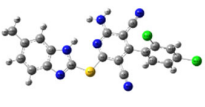
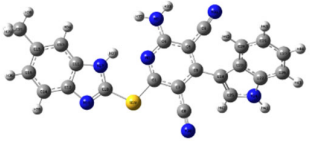
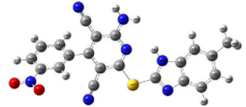
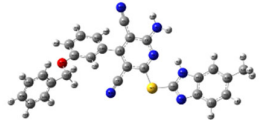
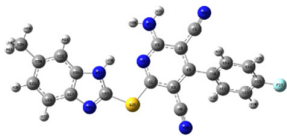
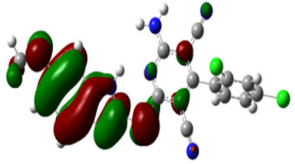
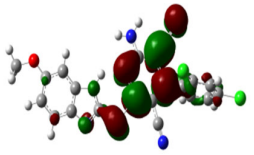
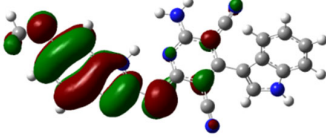
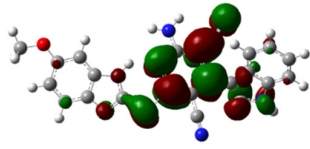
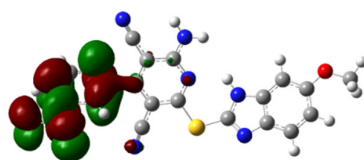
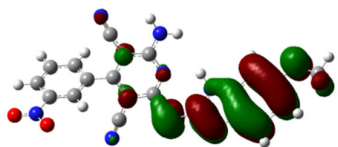
Compounds	Structure of optimized molecule	Compounds	Structure of optimized molecule
4a		4b	
4c		4d	
4e		4f	
4g		4h	
4i		4j	

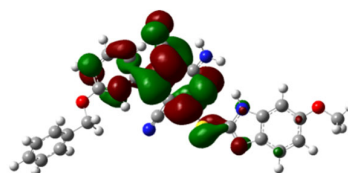
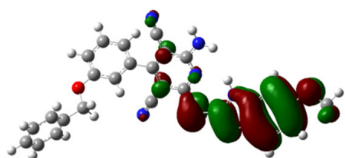
Table 7: HOMO LUMO structures of compounds **4(a-j)**

Compounds	Structure of HOMO	Structure of LUMO
4a		
4b		

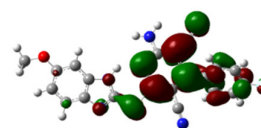
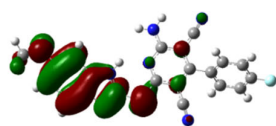
4c



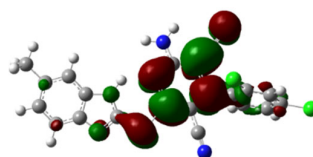
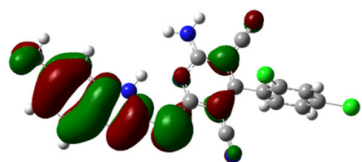
4d



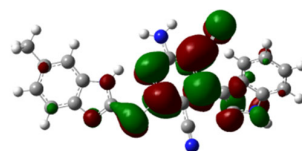
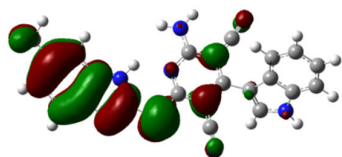
4e



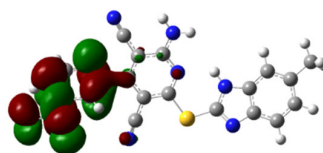
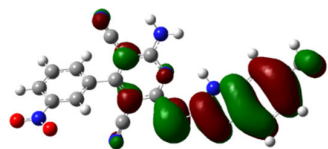
4f

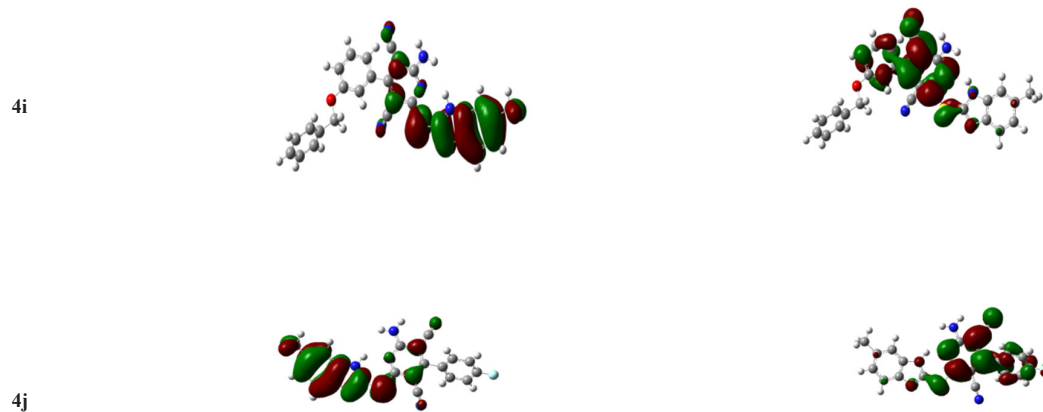


4g



4h



**Table 8.** MEP structures of compounds 4(a-j)

Compounds	MEP	Compounds	MEP
4a		4b	
4c		4d	
4e		4f	
4g		4h	
4i		4j	

Table 9. The quantum chemical parameters evaluated for **4(a-j)** compounds by DFT method B3LYP/6-311++G (d,p)

Electronic parameters	4a	4b	4c	4d	4e	4f	4g	4h	4i	4j
HOMO(eV)	-5.93	-5.75	-5.99	-5.84	-5.89	-6.21	-6.01	-6.27	-6.11	-6.18
LUMO(eV)	-2.63	-2.39	-3.14	-2.53	-2.65	-2.67	-2.42	-3.17	-2.56	-2.68
Energy gap(eV)	3.3	3.35	2.84	3.31	3.24	3.54	3.59	3.1	3.54	3.49
Dipole moment(D)	6.2	3.51	9.43	4.25	6.13	6.13	4.44	9.52	4.46	6.19
Electro negativity(χ)	1.65	1.68	1.42	1.65	1.62	1.77	1.79	1.55	1.77	1.75
Chemical potential(μ)	-1.65	-1.68	-1.42	-1.65	-1.62	-1.77	-1.79	-1.55	-1.77	-1.75
Chemical Hardness(η)	1.65	1.68	1.42	1.65	1.62	1.77	1.79	1.55	1.77	1.75
Chemical Softness(σ)	0.60	0.59	0.70	0.60	0.61	0.56	0.55	0.64	0.56	0.57
Nucleophilicity Index(N)	1.23	1.19	1.40	1.21	1.23	1.13	1.12	1.29	1.13	1.14
Electrophilicity index(ω)	0.81	0.84	0.71	0.82	0.81	0.88	0.89	0.77	0.88	0.87
Ionization potential(I)	5.93	5.75	5.99	5.84	5.89	6.21	6.01	6.27	6.11	6.18
Electron affinity(A)	2.63	2.39	3.14	2.53	2.65	2.67	2.42	3.17	2.56	2.68
Total energy (Hartree)	-1649	-	-1854	-1689	-	-	-	-	-	-

2.6. In silico ADMET studies

Physicochemical descriptors was evaluated through parameters such as molecular weight, number of rotatable bonds, H-Acceptor, H-Donor, Surface area, LogP, CaCO₂ Permeability, molecular refractivity, atom counts, Pgp-Inhibitor, HIA (%), PP-Binding (%), BBB, CYP2D₆ (inhibitor), Clearance, Half life and topological polar surface area (TPSA) of synthesized compounds **4(a-j)** and results are tabulated in **Table 10**.

Table 10. In silico ADMET screening of designed **4(a-j)** molecules

Attributes	4a	4b	4c	4d	4e	4f	4g	4h	4i	4j
Molecular Weight	467	437	443	504	416	451	427	426	487	399
number of rotatable bonds	4	4	5	7	4	3	3	4	6	3
TPSA (Å ²)	111.51	127.3	120.74	154.65	111.51	102.28	118.07	145.42	111.51	102.28
Molar refractivity	122.51	124.35	119.14	143.26	112.45	120.69	122.53	117.33	141.45	110.63
Total number of atoms	44	48	46	58	44	43	47	45	57	43
H-Acceptor	6	6	8	7	6	5	5	7	6	5
H-Donor	2	3	2	2	2	2	3	2	2	5
Surface area	124.40	437.11	167.54	133.63	124.40	115.17	130.96	158.31	98.38	115.17
Log P	5.09	4.21	3.85	5.11	4.04	5.42	4.51	4.14	5.89	4.36
CaCO ₂ Permeability	-5.07	-5.47	-5.08	-5.14	-4.95	-5.03	-5.44	-5.03	-5.30	-4.95
Pgp-Inhibitor*	+	-	+	+	+	+	+	+	+	+
HIA (%)	-	-	-	-	-	-	-	-	-	-
PP-Binding (%)	101.95	101.17	101.26	101.26	101.48	102.15	101.44	101.40	102.71	101.70
BBB	-	-	-	-	-	-	-	-	-	-
CYP2D6 (inhibitor)	-	+	-	-	-	-	+	-	-	-
Clearance	5.86	5.09	6.11	6.02	6.02	6.00	5.20	6.07	6.63	6.24
Half life	0.06	0.19	0.18	0.18	0.09	0.06	0.180	0.18	0.08	0.08

*+ =No, - =Yes

Because of the importance of pharmacokinetic features in therapeutic applications, pharmacokinetic estimation is considered the first stage in the development process. The drug-likeness profiles were calculated using Lipinski's (MW ≤ 500; HBA ≤ 10 and HBD ≤ 5), Ghose's (160 ≤ MW ≤ 480; 40 ≤ MR ≤ 130 and 20 ≤ atoms ≤ 70), Veber's (rotatable bonds ≤ 10 and TPSA ≤ 140), Egan's (TPSA ≤ 131.6), and Muegge (200 ≤ MW ≤ 600; number of aromatic rings ≤ 7)^{71,72}. **Table 11** shows the calculated drug-likeness features of the synthesized compounds. The compound **4d**, **4h** and **4i** violated more than one rule which may impact its drug-like properties, whereas rest of the compounds was found to violate not more than one rule. The Lipinski rule was followed by all the compounds whereas Muegge rule was violated by all the compounds. These findings indicate that compounds **4a**, **4b**, **4c**, **4e**, **4f**, **4g**, and **4j** have better drug like characteristics than rest of the compounds with good bioavailability which obeyed four filters (Lipinski, Ghose, Veber, and Egan) out of five.

Table 11. Drug likeness, of compounds **4(a-j)**

Compounds	Lipinski	Ghose	Veber	Egan	Muegge	Lipinski #violation	Ghose #violation	Veber #violation	Egan #violation	Muegge #violation
4a	Yes	Yes	Yes	Yes	No	0	0	0	0	1
4b	Yes	Yes	Yes	Yes	No	0	0	0	0	1
4c	Yes	Yes	Yes	Yes	No	0	0	0	0	1
4d	Yes	No	No	No	No	0	2	1	1	1
4e	Yes	Yes	Yes	Yes	No	0	0	0	0	1
4f	Yes	Yes	Yes	Yes	No	0	0	0	0	1
4g	Yes	Yes	Yes	Yes	No	0	0	0	0	1
4h	Yes	Yes	No	No	No	0	1	1	1	1
4i	Yes	No	Yes	Yes	No	0	1	0	0	1
4j	Yes	Yes	Yes	Yes	No	0	0	0	0	1

CaCO₂ permeability, Pgp inhibitor, and Pgp substrate were found to be in a reasonable range, with gastrointestinal absorption and no BBB crossing. The plasma protein binding of derivatives was shown to be greater than 90%, which affects the ligands' oral bioavailability and elimination (**Table 10**). The half-life and clearance of the medication exhibited a considerable range. The carcinogenicity of the target chemicals demonstrated that they are less hazardous. Metabolism influences both drug bioavailability and drug-drug interactions. Metabolism factors determine whether chemicals behave as a substrate or non-substrate for specific proteins. The substances (**4a-j**) were examined for metabolic characteristics, revealing that all (except **4b**) are P-gp substrates. The P-gp protein is vital in determining active efflux via biological membranes and cytochrome P₄₅₀ (CYP) enzymes⁷³. All of the compounds(except**4b** and **4h**) were determined to be CYP_{2D6} substrates (**Table 10**).

To determine if compounds were soluble in aqueous or non-aqueous conditions, the mean projected lipophilicity values were examined and determined using the consensus log P⁷¹. According to this, if a molecule is more soluble then its log P values will be more negative. Compounds (**4a-j**) were found to be insoluble in non-aqueous media. **Table 10** shows that the compounds were soluble in an aqueous solution based on log P values (log P <10 for poorly soluble, <6 for moderately soluble, <4 for soluble, <2 for extremely soluble, and <0 for very soluble).

The synthesized compounds **4(a-j)** were subjected to an *in silico* toxicity evaluation. Toxicological endpoints results suggested that all the compounds were predicted to be non-hepatotoxicity, non-immunotoxicity, non-cytotoxicity and non-carcinogenic. The toxicity class ranges from 1 to 6 are Class I: fatal if swallowed (LD₅₀ ≤ 5mg/kg) Class II: fatal if swallowed (5 mg/kg< LD₅₀ ≤ 50 mg/kg) Class III: toxic if swallowed (50 mg/kg< LD₅₀ ≤ 300 mg/kg) Class IV: harmful if swallowed (300 mg/kg< LD₅₀ ≤ 2000 mg/kg) Class V: non harmful if swallowed (2000 mg/kg< LD₅₀ ≤ 5000 mg/kg), Class VI: non-toxic (LD₅₀> 5000 mg/kg)⁷¹. The predicted LD₅₀ results suggested that the synthesized compounds were non-harmful if swallowed and belong to class V (**Table 12**)

Table 12. Toxicity study of the synthesized compounds **4(a-j)**

Compound	Hepatotoxicity	Immunotoxicity	Mutagenicity	AMES toxicity	Skin Sensitization	Carcinogenicity	Log LD ₅₀ (mg/kg)	Predicted Toxicity class
4a	Non-Toxic	Non-Toxic	Non-Toxic	Non-Toxic	Non-Toxic	Non-Toxic	3720	V
4b	Non-Toxic	Non-Toxic	Non-Toxic	Non-Toxic	Non-Toxic	Non-Toxic	3470	V
4c	Non-Toxic	Non-Toxic	Non-Toxic	Non-Toxic	Non-Toxic	Non-Toxic	3410	V
4d	Non-Toxic	Non-Toxic	Non-Toxic	Non-Toxic	Non-Toxic	Non-Toxic	3940	V
4e	Non-Toxic	Non-Toxic	Non-Toxic	Non-Toxic	Non-Toxic	Non-Toxic	3430	V
4f	Non-Toxic	Non-Toxic	Non-Toxic	Non-Toxic	Non-Toxic	Non-Toxic	3800	V
4g	Non-Toxic	Non-Toxic	Non-Toxic	Non-Toxic	Non-Toxic	Non-Toxic	3640	V
4h	Non-Toxic	Non-Toxic	Non-Toxic	Non-Toxic	Non-Toxic	Non-Toxic	3600	V
4i	Non-Toxic	Non-Toxic	Non-Toxic	Non-Toxic	Non-Toxic	Non-Toxic	4290	V
4j	Non-Toxic	Non-Toxic	Non-Toxic	Non-Toxic	Non-Toxic	Non-Toxic	3620	V

3. Conclusions

In this report, we have developed an effective protocol for the synthesis of some new 4-Amino-6-(1H-benzimidazol-2-ylsulfanyl)benzene-1,3-dicarbonitrile derivatives (**4a-j**) through catalyzed by ZnO nanoparticles and screened for their pharmacological and *in silico* investigations. We investigated the antimicrobial, cytotoxicity, anti-diabetic activities of all the 10 high-yield derivatives. In terms of cytotoxicity, compounds **4c** and **4h** were identified as the most promising molecules among the freshly synthesized ones. Compounds **4c** and **4h** outperformed the other compounds in terms of antibacterial activity. **4i** had the highest binding affinity of all the ligands, with a binding energy of -7.8 Kcal/mol and three hydrogen bonds, according to the *in silico* docking studies. Strong hydrogen bonds, hydrophobic interactions, and binding affinities were found in all other compounds too. ADMET profiles indicate that, our synthesized compounds obeyed five rules of drug likeness with good bioavailability. Pharmacokinetic parameters suggested that, our compounds have high GI absorption, no blood-brain permeant & less skin permeant. Hence there was no possibility of causing harmful toxicants. Lipophilicity based on LogP values indicated that the new derivatives were soluble in aqueous medium. Toxicological endpoints data revealed that all the compounds were expected to be non-hepatotoxic, non-immune toxic, non AMES toxic, non carcinogenic and non-cytotoxic in nature. The anticipated LD₅₀ result indicated that the produced chemicals were not harmful upon swallowing. The ten distinct benzimidazole derivatives (**4a-j**) synthesized in this study revealed a wide spectrum of biological activity, making it important pharmacophore in drug development.

Acknowledgements

The authors are thankful to the Chairman, Department of Industrial Chemistry, Kuvempu University, Shankaraghatta, for providing the laboratory facilities. The authors are also thankful to Mangalore University, Mangalore for providing the spectral data.

4. Experimental

4.1. Materials and methods

The synthesis was carried using high-purity analytical grade reagents, solvents, and compounds supplied from Sigma-Aldrich. Alumina TLC plates were used to monitor the reaction's progress. Ethyl acetate:hexane (1:4) was used as the mobile phase for TLC plates. A UV chamber was used to identify spots. The melting points were determined using electro thermal equipment with open capillary tubes (uncorrected). FTIR spectra were acquired on a Bruker spectrophotometer using KBr pellets in the 400–4000 cm^{-1} area. Using a Bruker spectrometer at 400 MHz and 100 MHz, respectively obtained the spectra for ^1H NMR and ^{13}C NMR. Chemical shifts (δ) were recorded in ppm relative to tetramethylsilane. The mass spectra of the compounds were validated using the LC-MS 2010, SHIMADZU mass analyzer.

4.2 Biological Studies

Various biological activities such as antibacterial activity, cytotoxicity, anti-diabetic activity, molecular docking, and DFT of newly synthesized compounds were performed systematically⁷⁴.

4.2.1 Antimicrobial activity

Samples were tested against two bacterial strains, gram-positive *Staphylococcus aureus* MTCC-7443 and gram-negative *Escherichia coli* MTCC-7410, as well as two fungal species, *Aspergillus flavus* MTCC-9606 and *Pichia anomala* MTCC-237. The inoculum was prepared with a concentration of 5×10^5 CFU/mL using sterile saline solution. As a stock solution, samples were dissolved in DMSO at a concentration of 20 mg/mL and deposited in various concentrations of 20, 40, 60, and 80g for separate wells. For bacteria, Muller Hinton agar was employed, while for fungi, Czapek's-Doxagar media was utilized. For bacteria, Rifampicin (30g) was employed as a positive control antibiotic, whereas Fluconazole (30g) was utilised for fungi. The diameter of the inhibitory zone (mm) was determined after 72 hours of incubation at 37 °C for bacteria and 28 °C for fungi.

4.2.2 Cytotoxicity property of synthesized compounds

4.2.2.1 Cell culture technique

The Human tumour cell line Hep G2 was provided by the National Centre for Cell Sciences (NCCS) in Pune, India. Cells were maintained in DMEM supplemented with 2mM l-glutamine and balanced salt solution (BSS) adjusted to contain 1.5g/L Na_2CO_3 , 0.1mM nonessential amino acids, 1mM sodium pyruvate, 2mM l-glutamine, 1.5g/L glucose, 10mM HEPES (4-(2-hydroxyethyl)-1-piperazine ethane sulfonic acid) and 10% fetal bovine serum (GIBCO, USA). The penicillin and streptomycin concentrations (100 IU/100 g) were adjusted to 1mL/L. The cells were maintained at 37°C with 5% CO_2 in a humidified CO_2 incubator.

4.2.2.2 Evaluation of cytotoxicity

An MTT test was used to calculate the inhibitory concentration (IC_{50}). Cultured cells (1×10^5) were sown in a 96-well plate and cultured at 37 °C in a 5% CO_2 incubator for 48 hours. After 48 hours, the monolayer was washed with media, and 100 μL of various test concentrations of samples were added to the monolayer, and the cells were incubated again under the same circumstances. After removing the growth medium, 100 μL of MTT solution was added to each well and incubated at 37 °C for 4 hours. Following the removal of the supernatant, 100 μL of DMSO was added to each well and incubated for 10 minutes to dissolve the formazan crystals. At 590nm, the optical density was observed. The percentage growth inhibition was calculated and results were expressed as IC_{50} values using dose-response curve.

Formula for % inhibition: $(\text{OD of blank} - \text{OD of test}) / \text{OD of Blank} \times 100$

Formula for IC_{50} was calculated by linear regression equation $Y = mX + b$

4.2.3 Anti-diabetic studies

4.2.3.1 α -Amylase inhibition properties

The α -amylase inhibition properties of samples were performed as described in Poovitha *et al.*, 2016⁷⁵. Porcine pancreatic α -amylase (3units/mL) was dissolved in 0.1 M phosphate buffered saline, pH 6.9. The different concentrations

of samples (0-125 µg/mL) were pre-incubated with enzyme for 10 min at 37°C. The reaction was initiated by adding substrate (0.1% starch) to the incubation medium. After 10 min incubation, the reaction was stopped by adding 250 µL dinitro salicylic (DNS) reagent (1% 3, 5-dinitrosalicylic acid, 0.2% phenol, 0.05% Na₂SO₃ and 1% NaOH in aqueous solution). The reaction was stopped by holding the reaction mixture in boiling water bath for 10 min. Thereafter, 250 µL of 40% potassium sodium tartrate solution was added the absorbance was recorded at 540 nm at room temperature. The percentage of inhibition was calculated by the formula: (OD of blank – OD of test/OD of Blank) *100 and the results were expressed in IC₅₀ values in comparison with Acarbose as a positive control.

4.3 Molecular docking

4.3.1 Preparation of ligand

The Ligands are drawn using ChemDraw software and the build of 3D structure and energy of each ligand was minimized using the USCF chimera tool by applying the AMBER force field and then ligands were converted into PDB format^{76,77}.

4.3.2 Preparation of the Receptor

The 3D crystal structure of VEGFR2 protein (PDB: 4AG8) was accessed through database (<https://www.rcsb.org>) and Co-crystal ligand was removed from protein. Using the USCF Chimera V2021 tool, optimization of hydrogen, refinement of protein, and minimization of energy were executed^{78,79}.

4.3.3 Docking and Visualization

Setting of a grid box around the active sites of proteins, designed ligands were docked against the receptor using AutodockVina in the PyRX workstation. The AutodockVina docking algorithm has been used to search for the best docked ligand and target conformation, Ligands with the lowest binding affinity will be considered as the best conformation, docked protein and target converted into pdb format by Schrödinger PyMol and interactions visualized Biovia Discovery studios⁸⁰⁻⁸⁵

4.3.4 DFT studies

DFT (Density functional theory) studies in Gaussian 09W software were performed on the synthesized compounds (**4a-4j**) using a hybrid functional B3LYP, which is a combination of Beckeexchange and LYP correlation functional^{86,87}, and basis set 6-311++G(d,p) was used for optimizations in gas phase. Using DFT studies, the total energies, Dipole moment, HOMO, LUMO, and band gap of the synthesized derivatives were calculated. The global parameters such as Electron affinity (A), Ionization potential (I), Mullikan electronegativity (χ), chemical potential (μ), chemical hardness (η), global electrophilicity index (ω) and MEP were calculated⁸⁸. To study the electronic properties of compounds (**4a-4j**), we first calculated HOMO (E_{HOMO}) and the LUMO (E_{LUMO}) energies. Using the value of E_{HOMO} and E_{LUMO} energy band gap can be estimated using following equation,

$$E_{L-H} = E_{LUMO} - E_{HOMO}$$

The HOMO and LUMO of compounds were used in determining of various global reactivity parameters such as ionization energy (I = -EHOMO), electron affinity (A = -ELUMO), chemical hardness (η = 1/2 (I - A)), chemical softness (σ = 1/η), electronegativity (χ = 1/2 (I + A)), chemical potential (μ = -χ), and electrophilicity index (ω = μ²/2η) to study about donor-acceptor interaction and intramolecular charge transfer (ICT) ability of synthesized compounds⁸⁹. Nucleophilicity index (N) is a Conceptual Density Functional Theory-based reactivity descriptor which was used to define variety of physicochemical behaviors⁹⁰. N is a measure of the electron donating power of an atom, molecule or ion and it is the inverse of electrophilicity index (ω)^{91,92}.

$$N = \frac{1}{\omega}$$

Electrophilicity index (ω) is the electron attracting power of the species and calculated the electrophilicity index by using equation

$$\omega = \frac{\mu^2}{2\eta} = \frac{\left[\frac{E_H + E_L}{2}\right]^2}{[E_L - E_H]}$$

where

μ = electron chemical potential

η = electron chemical hardness

E_H and E_L = Electron energies of frontier molecular orbital HUMO and LUMO

4.4 *In silico* ADMET studies

The pharmacokinetic properties of each target molecule were designed using the ADMET descriptor module via a web server (<https://admet.scbdd.com/>). This stage of the screening involved compounds with high binding energy values. Lipinski (2001), Ghose (1999), Veber (2002), Egan (2000), and Muegge (2001) Rules were used to assess the drug-likeness candidature of synthesized compounds⁷². A variety of ADMET descriptors, including LogP, CaCO₂ Permeability, molecular weight (MW), molecular refractivity (MR), atom counts, and topological polar surface area (TPSA), Plasma Protein Binding Percentage, CNS Blood-Brain Barrier, Cytochrome P₂D₆ models, and toxicity descriptors, such as Carcinogenicity, Half-life, and Drug Clearance, were used to predict pharmacokinetic properties^{80,93–95}.

4.5 Statistical analysis

Each experiment was carried out in triplicates, and the findings were reported as mean ± SE (standard error). The difference between the means of the groups was calculated using one way analysis of variance. The derivative results were compared to the control results. The P value < 0.01 was deemed statistically significant. R version 4.1.0 was used to perform all statistical analyses.

Supporting information

This includes materials, methods and spectra of the synthesized compounds (IR, ¹H NMR, ¹³C NMR, and LCMS).

Funding

The authors did not receive support from any organization for the submitted work.

Availability of data and material

The authors confirm that the data supporting the findings of this study are available within the article and its supplementary materials. The data sets generated during and analyzed during the current study are available from the corresponding author upon reasonable request.

Credit Authors statement

R Champa: Methodology, Investigation, and Writing Original Draft. **Vishnumurthy KA:** Supervision. **Yadav D Bodke:** Supervision, writing, & Editing. **HS Bhojya Naik:** Supervision. **IttePushphavathi:** DFT studies and software. **ND Satyanarayan, Nippu BN:** Molecular docking, ADME toxicology studies.

References

- Karaca Gençer, H., Acar Çevik, U., Levent, S., Sağlık, B.N., Korkut, B., Özkay, Y., Ilgın, S., and Öztürk, Y. (2017). New Benzimidazole-1,2,4-Triazole Hybrid Compounds: Synthesis, Anticandidal Activity and Cytotoxicity Evaluation. *Molecules* 22, 507. 10.3390/molecules22040507.
- Kazachenko, A.S., Tamış, E., Akman, F., Medimagh, M., Issaoui, N., Al-Dossary, O., Bousiakou, L.G., Kazachenko, A.S., Zimonin, D., and Skripnikov, A.M. (2022). A Comprehensive Study of N-Butyl-1H-Benzimidazole. *Molecules* 27, 7864. 10.3390/molecules27227864.
- Wubulikasimu, R., Yang, Y., Xue, F., Luo, X., Shao, D., Li, Y., Gao, R., and Ye, W. (2013). Synthesis and Biological Evaluation of Novel Benzimidazole Derivatives Bearing a Heterocyclic Ring at 4/5 Position. *Bull Korean Chem Soc* 34, 2297–2304. 10.5012/BKCS.2013.34.8.2297.
- Xiang, P., Zhou, T., Wang, L., Sun, C.-Y., Hu, J., Zhao, Y.-L., and Yang, L. (2012). Novel Benzothiazole, Benzimidazole and Benzoxazole Derivatives as Potential Antitumor Agents: Synthesis and Preliminary in Vitro Biological Evaluation. *Molecules* 17, 873–883. 10.3390/molecules17010873.
- Singh, M., and Tandon, V. (2011). Synthesis and biological activity of novel inhibitors of topoisomerase I: 2-Aryl-substituted 2-bis-1H-benzimidazoles. *Eur. J. Med. Chem.* 46, 659–669. 10.1016/j.ejmech.2010.11.046.
- Antoci, V., Cucu, D., Zbancioc, G., Moldoveanu, C., Mangalagiu, V., Amariuca-Mantu, D., Aricu, A., and Mangalagiu, I.I. (2020). Bis-(imidazole/benzimidazole)-pyridine derivatives: synthesis, structure and antimycobacterial activity. *Future Med. Chem.* 12, 207–222. 10.4155/fmc-2019-0063.
- Gobis, K., Foks, H., Serocki, M., Augustynowicz-Kopeć, E., and Napiórkowska, A. (2015). Synthesis and evaluation of in vitro antimycobacterial activity of novel 1H-benzo[d]imidazole derivatives and analogues. *Eur. J. Med. Chem.* 89, 13–20. 10.1016/j.ejmech.2014.10.031.

8. Awasthi, D., Kumar, K., Knudson, S.E., Slayden, R.A., and Ojima, I. (2013). SAR Studies on Trisubstituted Benzimidazoles as Inhibitors of *Mtb* FtsZ for the Development of Novel Antitubercular Agents. *J. Med. Chem.* 56, 9756–9770. 10.1021/jm401468w.
9. Morcoss, M.M., Abdelhafez, E.S.M.N., Ibrahim, R.A., Abdel-Rahman, H.M., Abdel-Aziz, M., and Abou El-Ella, D.A. (2020). Design, synthesis, mechanistic studies and in silico ADME predictions of benzimidazole derivatives as novel antifungal agents. *Bioorg. Chem.* 101, 103956. 10.1016/j.bioorg.2020.103956.
10. Padalkar, V.S., Borse, B.N., Gupta, V.D., Phatangare, K.R., Patil, V.S., Umape, P.G., and Sekar, N. (2016). Synthesis and antimicrobial activity of novel 2-substituted benzimidazole, benzoxazole and benzothiazole derivatives. *Arab. J. Chem.* 9, S1125–S1130. 10.1016/j.arabjc.2011.12.006.
11. Chandrika, N.T., Shrestha, S.K., Ngo, H.X., and Garneau-Tsodikova, S. (2016). Synthesis and investigation of novel benzimidazole derivatives as antifungal agents. *Bioorg. Med. Chem.* 24, 3680–3686. 10.1016/j.bmc.2016.06.010.
12. El-Gohary, N.S., and Shaaban, M.I. (2017). Synthesis and biological evaluation of a new series of benzimidazole derivatives as antimicrobial, anti-quorum-sensing and antitumor agents. *Eur. J. Med. Chem.* 131, 255–262. 10.1016/j.ejmech.2017.03.018.
13. Yadav, S., Narasimhan, B., and Kaur, H. (2016). Perspectives of Benzimidazole Derivatives as Anticancer Agents in the New Era. *ACAMC* 16, 1403–1425. 10.2174/1871520616666151103113412.
14. Ferro, S., Buemi, M.R., De Luca, L., Agharbaoui, F.E., Pannecouque, C., and Monforte, A.-M. (2017). Searching for novel N 1 -substituted benzimidazol-2-ones as non-nucleoside HIV-1 RT inhibitors. *Bioorg. Med. Chem.* 25, 3861–3870. 10.1016/j.bmc.2017.05.040.
15. Monforte, A.M., De Luca, L., Buemi, M.R., Agharbaoui, F.E., Pannecouque, C., and Ferro, S. (2018). Structural optimization of N1-aryl-benzimidazoles for the discovery of new non-nucleoside reverse transcriptase inhibitors active against wild-type and mutant HIV-1 strains. *Bioorg. Med. Chem.* 26, 661–674. 10.1016/j.bmc.2017.12.033.
16. Srivastava, R., Gupta, S.K., Naaz, F., Sen Gupta, P.S., Yadav, M., Singh, V.K., Singh, A., Rana, M.K., Gupta, S.K., Schols, D., et al. (2020). Alkylated benzimidazoles: Design, synthesis, docking, DFT analysis, ADMET property, molecular dynamics and activity against HIV and YFV. *Comput Biol Chem* 89, 107400. 10.1016/j.compbiolchem.2020.107400.
17. Veerasamy, R., Roy, A., Karunakaran, R., and Rajak, H. (2021). Structure–Activity Relationship Analysis of Benzimidazoles as Emerging Anti-Inflammatory Agents: An Overview. *Pharmaceuticals* 14, 663. 10.3390/ph14070663.
18. Baldisserotto, A., Demurtas, M., Lampronti, I., Tacchini, M., Moi, D., Balboni, G., Vertuani, S., Manfredini, S., and Onnis, V. (2020). In-Vitro Evaluation of Antioxidant, Antiproliferative and Photo-Protective Activities of Benzimidazolehydrazone Derivatives. *Pharmaceuticals* 13, 68. 10.3390/ph13040068.
19. Mariappan, G., Hazarika, R., Alam, F., Karki, R., Patangia, U., and Nath, S. (2015). Synthesis and biological evaluation of 2-substituted benzimidazole derivatives. *Arab. J. Chem.* 8, 715–719. 10.1016/j.arabjc.2011.11.008.
20. Brishty, S.R., Hossain, M.J., Khandaker, M.U., Faruque, M.R.I., Osman, H., and Rahman, S.M.A. (2021). A Comprehensive Account on Recent Progress in Pharmacological Activities of Benzimidazole Derivatives. *Front. Pharmacol.* 12, 762807. 10.3389/fphar.2021.762807.
21. Chojnacki, K., Wińska, P., Skierka, K., Wielechowska, M., and Bretner, M. (2017). Synthesis, in vitro antiproliferative activity and kinase profile of new benzimidazole and benzotriazole derivatives. *Bioorg. Chem.* 72, 1–10. 10.1016/j.bioorg.2017.02.017.
22. Gümrükçüoğlu, N. (2021). Synthesis and Antioxidant Properties of New Benzimidazole Derivatives. *Politeknik Dergisi* 24, 1699–1706. 10.2339/politeknik.718979.
23. Singh, V.K., and Parle, A. (2020). Synthesis, Characterization and Antioxidant Activity of 2-Aryl Benzimidazole Derivatives. *Asian J Pharm Res Dev* 8, 35–44. 10.22270/ajprd.v8i2.582.
24. Jian-Song, Gao, Q.-L., Wu, B.-W., Li, D., Shi, L., Zhu, T., Lou, J.-F., Jin, C.-Y., Zhang, Y.-B., Zhang, S.-Y., et al. (2019). Novel tertiary sulfonamide derivatives containing benzimidazole moiety as potent anti-gastric cancer agents: Design, synthesis and SAR studies. *Eur. J. Med. Chem.* 183, 111731. 10.1016/j.ejmech.2019.111731.
25. Bharadwaj, S.S., Poojary, B., Nandish, S.K.M., Kengaiyah, J., Kirana, M.P., Shankar, M.K., Das, A.J., Kulal, A., and Sannaningaiyah, D. (2018). Efficient Synthesis and in Silico Studies of the Benzimidazole Hybrid Scaffold with the Quinolinyloxadiazole Skeleton with Potential α -Glucosidase Inhibitory, Anticoagulant, and Antiplatelet Activities for Type-II Diabetes Mellitus Management and Treating Thrombotic Disorders. *ACS Omega* 3, 12562–12574. 10.1021/acsomega.8b01476.
26. Siddig, L.A., Khasawneh, M.A., Samadi, A., Saadeh, H., Abutaha, N., and Wadaan, M.A. (2021). Synthesis of novel thiourea-urea-benzimidazole derivatives as anticancer agents. *Open Chem.* 19, 1062–1073. 10.1515/chem-2021-0093.
27. Sharma, K., Shrivastava, A., Mehra, R.N., Deora, G.S., Alam, M.M., Zaman, M.S., and Akhter, M. (2018). Synthesis of novel benzimidazole acrylonitriles for inhibition of *Plasmodium falciparum* growth by dual target inhibition. *Arch. Pharm. Chem. Life Sci.* 351, 1700251. 10.1002/ardp.201700251.
28. Mueller, R., Reddy, V., Nchinda, A.T., Mebrahtu, F., Taylor, D., Lawrence, N., Tanner, L., Barnabe, M., Eyermann, C.J., Zou, B., et al. (2020). Lerisetron Analogues with Antimalarial Properties: Synthesis, Structure–Activity Relationship Studies, and Biological Assessment. *ACS Omega* 5, 6967–6982. 10.1021/acsomega.0c00327.
29. Lee, Y.T., Tan, Y.J., and Oon, C.E. (2023). Benzimidazole and its derivatives as cancer therapeutics: The potential role from traditional to precision medicine. *Acta Pharm. Sin. B* 13, 478–497. 10.1016/j.apsb.2022.09.010.

30. Jasiński, R. (2015). A stepwise, zwitterionic mechanism for the 1,3-dipolar cycloaddition between (Z)-C-4-methoxyphenyl-N-phenylnitron and gem-chloronitroethene catalysed by 1-butyl-3-methylimidazolium ionic liquid cations. *Tetrahedron Lett.* 56, 532–535. 10.1016/j.tetlet.2014.12.007.
31. Jasiński, R. (2023). On the question of selective protocol for the preparation of juglone via (4+2) cycloaddition involving 3-hydroxypyridazine: DFT mechanistic study. *Chem Heterocycl Comp* 59, 179–182. 10.1007/s10593-023-03180-4.
32. Kras, J., Sadowski, M., Zawadzińska, K., Nagatsky, R., Woliński, P., Kula, K., and Łapczuk, A. (2023). Thermal [3+2] cycloaddition reactions as most universal way for the effective preparation of five-membered nitrogen containing heterocycles. *Sci. Rad.* 2, 247–267. 10.58332/scirad2023v2i3a03.
33. Sadowski, M., Utnicka, J., Wójtowicz, A., and Kula, K. (2023). The global and local Reactivity of C,N-diarylnitryle imines in [3+2] cycloaddition processes with trans- β -nitrostyrene according to Molecular Electron Density Theory: A computational study. *Curr. Chem. Lett.* 12, 421–430. 10.5267/j.ccl.2022.11.004.
34. Kula, K., and Łapczuk-Krygier, A. (2018). A DFT computational study on the [3+2] cycloaddition between parent thionitron and nitroethene. *Curr. Chem. Lett.* 27–34. 10.5267/j.ccl.2018.02.001.
35. Zawadzińska, K., and Kula, K. (2021). Application of β -Phosphorylated Nitroethenes in [3+2] Cycloaddition Reactions Involving Benzonitrile N-Oxide in the Light of a DFT Computational Study. *Organics* 2, 26–37. 10.3390/org2010003.
36. Sadowski, M., and Kula, K. (2024). Nitro-functionalized analogues of 1,3-Butadiene: An overview of characteristic, synthesis, chemical transformations and biological activity. *Curr. Chem. Lett.* 13, 15–30. 10.5267/j.ccl.2023.9.003.
37. Boguszewska-Czubarra, A., Kula, K., Wnorowski, A., Biernasiuk, A., Popiolek, L., Miodowski, D., Demchuk, O.M., and Jasiński, R. (2019). Novel functionalized β -nitrostyrenes: Promising candidates for new antibacterial drugs. *Saudi Pharm J* 27, 593–601. 10.1016/j.jsps.2019.02.007.
38. Pathare, B., and Bansode, T. (2021). Review- biological active benzimidazole derivatives. *Results Chem* 3, 100200. 10.1016/j.rechem.2021.100200.
39. Küçükbay, H., Uçkun, M., Apohan, E., and Yeşilada, Ö. (2021). Cytotoxic and antimicrobial potential of benzimidazole derivatives. *Arch Pharm* 354, 2100076. 10.1002/ardp.202100076.
40. Blanckaert, P., Cannaert, A., Van Uytfanghe, K., Hulpia, F., Deconinck, E., Van Calenbergh, S., and Stove, C. (2020). Report on a novel emerging class of highly potent benzimidazole NPS opioids: Chemical and in vitro functional characterization of isotonitazene. *Drug Test Anal* 12, 422–430. 10.1002/dta.2738.
41. Alaqeel, S.I. (2017). Synthetic approaches to benzimidazoles from o-phenylenediamine: A literature review. *J. Saudi Chem. Soc.* 21, 229–237. 10.1016/j.jscs.2016.08.001.
42. Morais, G.R., Palma, E., Marques, F., Gano, L., Oliveira, M.C., Abrunhosa, A., Miranda, H.V., Outeiro, T.F., Santos, I., and Paulo, A. (2017). Synthesis and Biological Evaluation of Novel 2-Aryl Benzimidazoles as Chemotherapeutic Agents: Fluoroalkylated 2-Aryl Benzimidazoles as Lead Candidates for the Generation of Chemotherapeutic Agents. *J. Heterocyclic Chem.* 54, 255–267. 10.1002/jhet.2575.
43. Bugday, N., Kucukbay, F.F.Z., Apohan, E., Kucukbay, H., Serindag, A., and Yesilada, O. (2017). Synthesis and Evaluation of Novel Benzimidazole Conjugates Incorporating Amino Acids and Dipeptide Moieties. *LOC* 14, 198–206. 10.2174/1570178614666170203093406.
44. Yılmaz, Ü., Küçükbay, H., Deniz, S., and Şireci, N. (2013). Synthesis, Characterization and Microwave-Promoted Catalytic Activity of Novel N-phenylbenzimidazolium Salts in Heck-Mizoroki and Suzuki-Miyaura Cross-Coupling Reactions under Mild Conditions. *Molecules* 18, 2501–2517. 10.3390/molecules18032501.
45. Bektaş, H., Sökmen, B.B., Aydın, S., Menteşe, E., Bektaş, A., and Dilekçi, G. (2020). Design, synthesis, and characterization of some new benzimidazole derivatives and biological evaluation. *Journal of Heterocyclic Chem* 57, 2234–2242. 10.1002/jhet.3943.
46. Mulugeta, E., and Samuel, Y. (2022). Synthesis of Benzimidazole-Sulfonyl Derivatives and Their Biological Activities. *Biochem. Res. Int.* 2022, 1–13. 10.1155/2022/7255299.
47. Chari, M.A., Zaid-A-Mosaa, Shobha, D., and Malayalama, S. (2013). Synthesis of Multifunctionalised 2-Substituted Benzimidazoles Using Copper (II) Hydroxide as Efficient Solid Catalyst. *IJOC* 03, 243–250. 10.4236/ijoc.2013.34035.
48. Adharvana Chari, M., Shobha, D., and Sasaki, T. (2011). Room temperature synthesis of benzimidazole derivatives using reusable cobalt hydroxide (II) and cobalt oxide (II) as efficient solid catalysts. *Tetrahedron Lett.* 52, 5575–5580. 10.1016/j.tetlet.2011.08.047.
49. Chung, N.T., Dung, V.C., and Duc, D.X. (2023). Recent achievements in the synthesis of benzimidazole derivatives. *RSC Adv.* 13, 32734–32771. 10.1039/D3RA05960J.
50. Kim, Y., and Li, C.-J. (2020). Perspectives on green synthesis and catalysis. *Green Synthesis and Catalysis* 1, 1–11. 10.1016/j.gresc.2020.06.002.
51. Sachdeva, H., and Saroj, R. (2013). ZnO Nanoparticles as an Efficient, Heterogeneous, Reusable, and Ecofriendly Catalyst for Four-Component One-Pot Green Synthesis of Pyranopyrazole Derivatives in Water. *Sci. World J.* 2013, 1–8. 10.1155/2013/680671.
52. Mohammed, S.M., Shehab, W.S., Emwas, A.-H.M., Jaremko, M., Abdellattif, M.H., Zordok, W.A., and Tantawy, E.S. (2023). Eco-Friendly Synthesis of 1H-benzo[d]imidazole Derivatives by ZnO NPs Characterization, DFT Studies, Antioxidant and Insilico Studies. *Pharmaceuticals* 16, 969. 10.3390/ph16070969.
53. Alinezhad, H., Salehian, F., and Biparva, P. (2012). Synthesis of Benzimidazole Derivatives Using Heterogeneous ZnO Nanoparticles. *Synth. Commun.* 42, 102–108. 10.1080/00397911.2010.522294.

54. Paul, B., Vadivel, S., Dhar, S.S., Debbarma, S., and Kumaravel, M. (2017). One-pot green synthesis of zinc oxide nano rice and its application as sonocatalyst for degradation of organic dye and synthesis of 2-benzimidazole derivatives. *J. Phys. Chem. Sol.* *104*, 152–159. 10.1016/j.jpcs.2017.01.007.
55. Hao, D., Yun-lei, Z., Xiao-peng, S., Jin-ming, Y., and Dong, F. (2014). Synthesis of 2-amino-4-phenyl-6-(phenylsulfanyl)-3,5-dicyanopyridines by tandem reaction. *Res. Chem. Intermed.* *40*, 587–594. 10.1007/s11164-012-0984-0.
56. Raoufi, D. (2013). Synthesis and microstructural properties of ZnO nanoparticles prepared by precipitation method. *Renewable Energy* *50*, 932–937. 10.1016/j.renene.2012.08.076.
57. Özkay, Y., Tunali, Y., Karaca, H., and Işıklıdağ, İ. (2011). Antimicrobial activity of a new series of benzimidazole derivatives. *Arch. Pharm. Res.* *34*, 1427–1435. 10.1007/s12272-011-0903-8.
58. Aroua, L.M., Alosaimi, A.H., Alminderej, F.M., Messaoudi, S., Mohammed, H.A., Almahmoud, S.A., Chigurupati, S., Albadri, A.E.A.E., and Mekni, N.H. (2023). Synthesis, Molecular Docking, and Bioactivity Study of Novel Hybrid Benzimidazole Urea Derivatives: A Promising α -Amylase and α -Glucosidase Inhibitor Candidate with Antioxidant Activity. *Pharmaceutics* *15*, 457. 10.3390/pharmaceutics15020457.
59. Sukanya, S.H., Venkatesh, T., Aditya Rao, S.J., and Joy, M.N. (2022). Efficient L-Proline catalyzed synthesis of some new (4-substituted-phenyl)-1,5-dihydro-2H-pyrimido[4,5-d][1,3]thiazolo[3,2a]-pyrimidine-2,4(3H)-diones bearing thiazolopyrimidine derivatives and evaluation of their pharmacological activities. *J. Mol. Struct.* *1247*, 131324. 10.1016/j.molstruc.2021.131324.
60. Cheke, R.S., Patil, V.M., Firke, S.D., Ambhore, J.P., Ansari, I.A., Patel, H.M., Shinde, S.D., Pasupuleti, V.R., Hassan, M.I., Adnan, M., et al. (2022). Therapeutic Outcomes of Isatin and Its Derivatives against Multiple Diseases: Recent Developments in Drug Discovery. *Pharmaceutics* *15*, 272. 10.3390/ph15030272.
61. Haredi Abdelmonsef, A., Eldeeb Mohamed, M., El-Naggat, M., Temairk, H., and Mohamed Mosallam, A. (2020). Novel Quinazolin-2,4-Dione Hybrid Molecules as Possible Inhibitors Against Malaria: Synthesis and in silico Molecular Docking Studies. *Front. Mol. Biosci.* *7*, 105. 10.3389/fmolb.2020.00105.
62. Furman, D., Campisi, J., Verdin, E., Carrera-Bastos, P., Targ, S., Franceschi, C., Ferrucci, L., Gilroy, D.W., Fasano, A., Miller, G.W., et al. (2019). Chronic inflammation in the etiology of disease across the life span. *Nat Med* *25*, 1822–1832. 10.1038/s41591-019-0675-0.
63. Mantovani, A., Marchesi, F., Porta, C., Sica, A., and Allavena, P. (2007). Inflammation and cancer: Breast cancer as a prototype. *The Breast* *16*, 27–33. 10.1016/j.breast.2007.07.013.
64. Montfort, A., Colacios, C., Levade, T., Andrieu-Abadie, N., Meyer, N., and Ségui, B. (2019). The TNF Paradox in Cancer Progression and Immunotherapy. *Front. Immunol.* *10*, 1818. 10.3389/fimmu.2019.01818.
65. Ali, A., Khalid, M., Rehman, M.F.U., Haq, S., Ali, A., Tahir, M.N., Ashfaq, M., Rasool, F., and Braga, A.A.C. (2020). Efficient Synthesis, SC-XRD, and Theoretical Studies of *O*-Benzenesulfonylated Pyrimidines: Role of Noncovalent Interaction Influence in Their Supramolecular Network. *ACS Omega* *5*, 15115–15128. 10.1021/acsomega.0c00975.
66. Ögretir, C., and Kanişkan, N. (1993). Frontier Orbital Theory and Chemical Reactivity: The Utility of Spectroscopy and Molecular Orbital Calculations. In *Recent Experimental and Computational Advances in Molecular Spectroscopy*, R. Fausto, ed. (Springer Netherlands), pp. 351–367. 10.1007/978-94-011-1974-0_20.
67. Koopmans, T. (1934). Über die Zuordnung von Wellenfunktionen und Eigenwerten zu den Einzelnen Elektronen Eines Atoms. *Physica* *1*, 104–113. 10.1016/S0031-8914(34)90011-2.
68. Matada, M.N., Jathi, K., Malingappa, P., and Pushpavathi, I. (2020). Synthesis, spectroscopic, DFT and electrochemical studies of heterocyclic azo dyes derived from 1-[(E)-benzylideneamino](phenyl)methyl} naphthalen-2-ol. *Chem. Data Coll.* *25*, 100314. 10.1016/j.cdc.2019.100314.
69. Conradie, J. (2022). Redox Chemistry of tris(β -diketonate)cobalt(III) Complexes: A Molecular View. *J. Electrochem. Soc.* *169*, 046522. 10.1149/1945-7111/ac6705.
70. Parr, R.G., Szentpály, L.V., and Liu, S. (1999). Electrophilicity Index. *J. Am. Chem. Soc.* *121*, 1922–1924. 10.1021/ja983494x.
71. Megha, G.V., Bodke, Yadav.D., and Shanavaz, H. (2023). Synthesis of novel 2, 5-disubstituted tetrazole derivatives as potent biological agents. *Curr. Chem. Lett.* *12*, 397–412. 10.5267/j.ccl.2022.11.006.
72. Ononamadu, C., and Ibrahim, A. (2021). Molecular docking and prediction of ADME/drug-likeness properties of potentially active antidiabetic compounds isolated from aqueous-methanol extracts of *Gymnema sylvestris* and *Combretum micranthum*. *bta* *102*, 85–99. 10.5114/bta.2021.103765.
73. Pal, D., Kwatra, D., Minocha, M., Paturi, D.K., Budda, B., and Mitra, A.K. (2011). Efflux transporters- and cytochrome P-450-mediated interactions between drugs of abuse and antiretrovirals. *Life Sci.* *88*, 959–971. 10.1016/j.lfs.2010.09.012.
74. Champa, R., Vishnumurthy, K.A., Bodke, Y.D., Bhojya Naik, H.S., Pushpavathi, I., Meghana, P., and Kadam, P.R. (2023). Synthesis, characterization, and biological investigations of potentially bioactive heterocyclic compounds containing benzimidazole nucleus. *Results Chem.* *6*, 101018. 10.1016/j.rechem.2023.101018.
75. Poovitha, S., and Parani, M. (2016). In vitro and in vivo α -amylase and α -glucosidase inhibiting activities of the protein extracts from two varieties of bitter melon (*Momordica charantia* L.). *BMC Complement Altern Med* *16*, 185. 10.1186/s12906-016-1085-1.
76. N., N.B., R., S.K.J., Rahman, A., Kumaraswamy, H., and Satyanarayan, N. (2022). Design and synthesis of novel tetrazoloquinoline bridged isatin derivatives as potential anticancer leads against MIA PaCa-2 human pancreatic cancer cell line. *J. Mol. Struct.* *1263*, 133103. 10.1016/j.molstruc.2022.133103.

77. Anjan Kumar, G.C., Bodke, Y.D., Manjunatha, B., Satyanarayan, N.D., Nippu, B.N., and Joy, M.N. (2022). Novel synthesis of 3-(Phenyl) (ethylamino) methyl-4-hydroxy-2H-chromen-2-one derivatives using biogenic ZnO nanoparticles and their applications. *Chim.Tech.Acta* 9, 20229104, 5495. 10.15826/chimtech.2022.9.1.04.
78. McTigue, M., Murray, B.W., Chen, J.H., Deng, Y.-L., Solowiej, J., and Kania, R.S. (2012). Molecular conformations, interactions, and properties associated with drug efficiency and clinical performance among VEGFR TK inhibitors. *Proc. Natl. Acad. Sci. U.S.A.* 109, 18281–18289. 10.1073/pnas.1207759109.
79. Pettersen, E.F., Goddard, T.D., Huang, C.C., Couch, G.S., Greenblatt, D.M., Meng, E.C., and Ferrin, T.E. (2004). UCSF Chimera?A visualization system for exploratory research and analysis. *J. Comput. Chem.* 25, 1605–1612. 10.1002/jcc.20084.
80. B N, N., Rahman, A., Jain R, S.K., K S, M., Kumaraswamy, H.M., Mahadevan, K.M., and Satyanarayan, N.D. (2023). Design, Synthesis and Anticancer Screening of Cu-Catalyzed SnAr Substituted Pyridine Bridged Ring Systems. *J. Mol. Struct.* 1277, 134829. 10.1016/j.molstruc.2022.134829.
81. Gaillard, T. (2018). Evaluation of AutoDock and AutoDock Vina on the CASF-2013 Benchmark. *J. Chem. Inf. Model.* 58, 1697–1706. 10.1021/acs.jcim.8b00312.
82. Dallakyan, S., and Olson, A.J. (2015). Small-Molecule Library Screening by Docking with PyRx. In *Chemical Biology Methods in Molecular Biology.*, J. E. Hempel, C. H. Williams, and C. C. Hong, eds. (Springer New York), pp. 243–250. 10.1007/978-1-4939-2269-7_19.
83. Rigsby, R.E., and Parker, A.B. (2016). Using the PyMOL application to reinforce visual understanding of protein structure: PyMOL Application to Understand Protein Structure. *Biochem. Mol. Biol. Educ.* 44, 433–437. 10.1002/bmb.20966.
84. Rahman, A., N, P., N, N.B., Kumaraswamy, H.M., Rajeshwara, A.N., and Satyanarayan, N.D. (2022). Synthesis and anticancer screening of some novel Pd-catalysed 3-methyl indole based analogues on Mia PaCa-2 cell line. *J. Mol. Struct.* 1264, 133211. 10.1016/j.molstruc.2022.133211.
85. Patil, P., Yadav, A., Bavkar, L., N, N.B., Satyanarayan, N.D., Mane, A., Gurav, A., Hangirgekar, S., and Sankpal, S. (2021). [MerDABCO-SO₃H]Cl catalyzed synthesis, antimicrobial and antioxidant evaluation and molecular docking study of pyrazolopyranopyrimidines. *J. Mol. Struct.* 1242, 130672. 10.1016/j.molstruc.2021.130672.
86. Becke, A.D. (1988). Density-functional exchange-energy approximation with correct asymptotic behavior. *Phys. Rev. A* 38, 3098–3100. 10.1103/PhysRevA.38.3098.
87. Lee, C., Yang, W., and Parr, R.G. (1988). Development of the Colle-Salvetti correlation-energy formula into a functional of the electron density. *Phys. Rev. B* 37, 785–789. 10.1103/PhysRevB.37.785.
88. Nagaraja, O., Bodke, Y.D., Pushpavathi, I., and Ravi Kumar, S. (2020). Synthesis, characterization and biological investigations of potentially bioactive heterocyclic compounds containing 4-hydroxy coumarin. *Heliyon* 6, e04245. 10.1016/j.heliyon.2020.e04245.
89. Pandith, A., and Seo, Y.J. (2020). Label-free sensing platform for miRNA-146a based on chromo-fluorogenic pyrophosphate recognition. *J. Inorg. Biochem.* 203, 110867. 10.1016/j.jinorgbio.2019.110867.
90. Yadav, P., Tandon, H., Malik, B., and Chakraborty, T. (2022). A New Approach to Find Out the Correlation Between Nucleophilicity Index (N) and Hammett Constant. *Acta Pharmacol. Sin.* 3, 13–16.
91. Chattaraj, P.K., and Maiti, B. (2001). Reactivity Dynamics in Atom-Field Interactions: A Quantum Fluid Density Functional Study. *J. Phys. Chem. A* 105, 169–183. 10.1021/jp0019660.
92. Pratihari, S., and Roy, S. (2010). Nucleophilicity and Site Selectivity of Commonly Used Arenes and Heteroarenes. *J. Org. Chem.* 75, 4957–4963. 10.1021/jo100425a.
93. Prasad, S.R., Satyanarayan, N.D., Shetty, A.S.K., and Thippeswamy, B. (2022). Synthesis, antimicrobial, and antitubercular evaluation of new Schiff bases with in silico ADMET and molecular docking studies. *Eur. J. Chem.* 13, 109–116. 10.5155/eurjchem.13.1.109-116.2216.
94. Kadam, P.R., Bodke, Y.D., B, Manjunatha., Pushpavathi, Itte., Satyanarayan, N.D., and Nippu, B.N. (2023). Synthesis, characterization, DFT and biological study of new methylene thio-linked coumarin derivatives. *J. Mol. Struct.* 1278, 134918. 10.1016/j.molstruc.2023.134918.
95. Kadam, P.R., Bodke, Y.D., Naik, M.D., Nagaraja, O., and Manjunatha, B. (2022). One-pot three-component synthesis of thioether linked 4-hydroxycoumarin-benzothiazole derivatives under ambient condition and evaluation of their biological activity. *Results Chem* 4, 100303. 10.1016/j.rechem.2022.100303.

